

A new Triassic-Jurassic section in the southern part of the Holy Cross Mts. (Poland) – implications for palaeogeography

Małgorzata KOZŁOWSKA¹*, Marcin BARSKI¹, Radosław MIESZKOWSKI¹
and Katarzyna ANTOSZEWSKA¹

¹ University of Warsaw, Institute of Geology, Faculty of Geology, wirki i Wigury 93, 02-089 Warszawa, Poland

Kozłowska, M., Barski, M., Mieszkowski, R., Antoszevska, K., 2016. A new Triassic-Jurassic section in the southern part of the Holy Cross Mts. (Poland) – implications for palaeogeography. *Geological Quarterly*, **60** (2): 365–484, doi: 10.7306/gq.1259



Sedimentological, stratigraphical and geophysical studies across a new Triassic-Jurassic transition section in the Holy Cross Mts., Poland have revealed a large sedimentary hiatus embracing the entire latest Triassic–Early Jurassic – earliest Middle Jurassic time interval and yielded new data on the Triassic fluvial system and on Middle Jurassic shallow marine sedimentation. The presence of organic-walled dinoflagellate cysts allowed a precise age assignment of the black clay facies. Regional discussions and comparisons may be made with other areas with a similar depositional environment in Poland. For the first time a counterpart of the “Kocieliskie Beds” lithostratigraphic unit is proposed to exist in the Holy Cross Mts. area.

Key words: Middle Jurassic transgression, dinoflagellate cysts, stratigraphy, electrical resistivity tomography (ERT).

INTRODUCTION

The lithology and thickness of the Permian-Mesozoic succession in the Holy Cross Mountains (HCM) in central Poland is regionally variable. One of the most diverse intervals in the succession, widely discussed in the literature, is the Triassic-Jurassic transition (Lewiński, 1912; Karaszewski, 1962; Jurkiewiczowa, 1967; Siemińska, 1967; Karaszewski and Kopik, 1970; Kopik, 1970; Piekosiński, 1983, 2004; Deczkowski, 1997; Piekosiński et al., 2014). Generally, to the north of the HCM Fold Belt, the Upper Triassic red- and vari-coloured terrestrial deposits (Keuper) are subdivided into several informal formations (see Piekosiński, 2009). The Upper Triassic rocks are generally conformably overlain by thick (up to 900 m) continental and marginal marine deposits of the Lower Jurassic siliciclastic succession, with the Upper Rhaetian to Lower Hettangian Zagaje Formation of fluvial and lacustrine origin at the base (Piekosiński, 2004). To the south of the HCM Fold Belt, the Upper Triassic red, fine-grained clastics are directly overlain by Middle Jurassic transgressive marine sedimentary strata (Lewiński, 1912; Siemińska, 1967, 1969; Barski, 1999). In the southern region the rocks representing the uppermost Triassic, Lower Jurassic and the lower part of the Middle Jurassic have probably been removed by erosion. However, they are preserved in the western part of the Mesozoic margin of the HCM (= MHCM), where the Lower Jurassic is represented by gravels and coarse-

-grained gravelly sandstones, referred to the Snochowice Beds (Dadlez, 1962; Jurkiewiczowa, 1967), included by Piekosiński (2004) within the Zagaje Formation, and covered by younger deposits of the Zagaje Formation. The Snochowice Beds have a thickness increasing rapidly to the north, from zero up to seventy metres, and further towards the north and north-west they interfinger with finer-grained deposits of the Zagaje Formation. The variegated thickness of the Snochowice Beds was firstly explained as a result of accumulation in river valleys (Jurkiewiczowa, 1967). Piekosiński (2004) also interpreted them as braided-river deposits. The Snochowice Beds thickness pattern, facies development, and lateral distribution suggest an alluvial fan origin with a synsedimentary wedge-shaped geometry (Piekosiński, 2004; Kozłowska, 2012). The alluvial fan formation is interpreted as a result of the development of significant relief on the previously flat basin floor (Jurkiewiczowa, 1967; Kozłowska, 2012). The pronounced lithological differentiation of the Triassic-Jurassic transition in the transect discussed is related to faulting and re-arrangement of the basin floor in Late Triassic times (Pawłowska, 1979; Deczkowski and Franczyk, 1988; Brański, 2004; Kozłowska, 2012). The diverse scale of tectonic uplift presumably caused differential partial erosion of the Upper Triassic rocks in the southern and western part of the area (Jurkiewiczowa, 1967; Deczkowski and Franczyk, 1988). The Upper Triassic succession is referred herein to the Keuper (Piekosiński, 2009), although the upper boundary is still not clearly defined in the area studied (Kopik, 1970; Senkiewiczowa, 1970; Pawłowska, 1979; Deczkowski and Franczyk, 1988; Fijałkowska, 1992; Krupnik et al., 2014).

The timing of the Middle Jurassic marine transgressions onto the southeastern part of the Polish epicontinental basin is widely discussed in the literature (Siemińska, 1969;

* Corresponding author, e-mail: mmkzłowska@uw.edu.pl

Daniec, 1970; Siemi tkowska-Gi ejewska, 1974; Dayczak-Calikowska and Moryc, 1988; Feldman-Olszewska, 1997). To the south of the HCM Fold Belt (e.g., Wola Morawicka section), the oldest Jurassic marine deposits are represented by Lower Bathonian black mudstones (Siemi tkowska, 1967; Barski, 1999). However, in some places, e.g. the Brzegi IG 1 borehole (Jurkiewicz, 1974) and Gumienice exposure (Siemi tkowska, 1969), transgressive sandstone beds occur below biostratigraphically dated Bathonian or Callovian rocks. The pre-Bajocian/Bathonian transgression morphology was probably driven by uplift linked to the initial rifting processes of the Tethys Ocean postulated by Matyja (2015).

This paper describes the sedimentological and palaeogeographical characteristics of the new section of Triassic and Jurassic deposits in the recently exposed Wolica section in the southern part of the MHCM.

Detailed sedimentological analyses carried out at the exposures were supplemented with electrical resistivity tomography (ERT) data, allowing interpretation of the depositional geometry

of the rocks analysed and reconstruction of the geological history of the study area, especially focused on the character of the Middle Jurassic transgression.

GEOLOGICAL SETTING

Permian to Cretaceous rocks, cropping out around the HCM Fold Belt in central Poland (Fig. 1), represent a succession of sedimentary rocks about 5 km thick that infill the southeastern part of the Polish epicontinental basin (Kutek and Głazek, 1972), linked until the Middle Jurassic with the Danish Basin and later with the Central European Basin System (Pie kowski et al., 2008). The rocks are referred to in the literature as the MHCM, due to the present-day map resulting from post-Alpine inversion of the basin and local exhumation of the underlying Paleozoic rocks largely deformed by Variscan folding (Kutek and Głazek, 1972; Fig. 1).

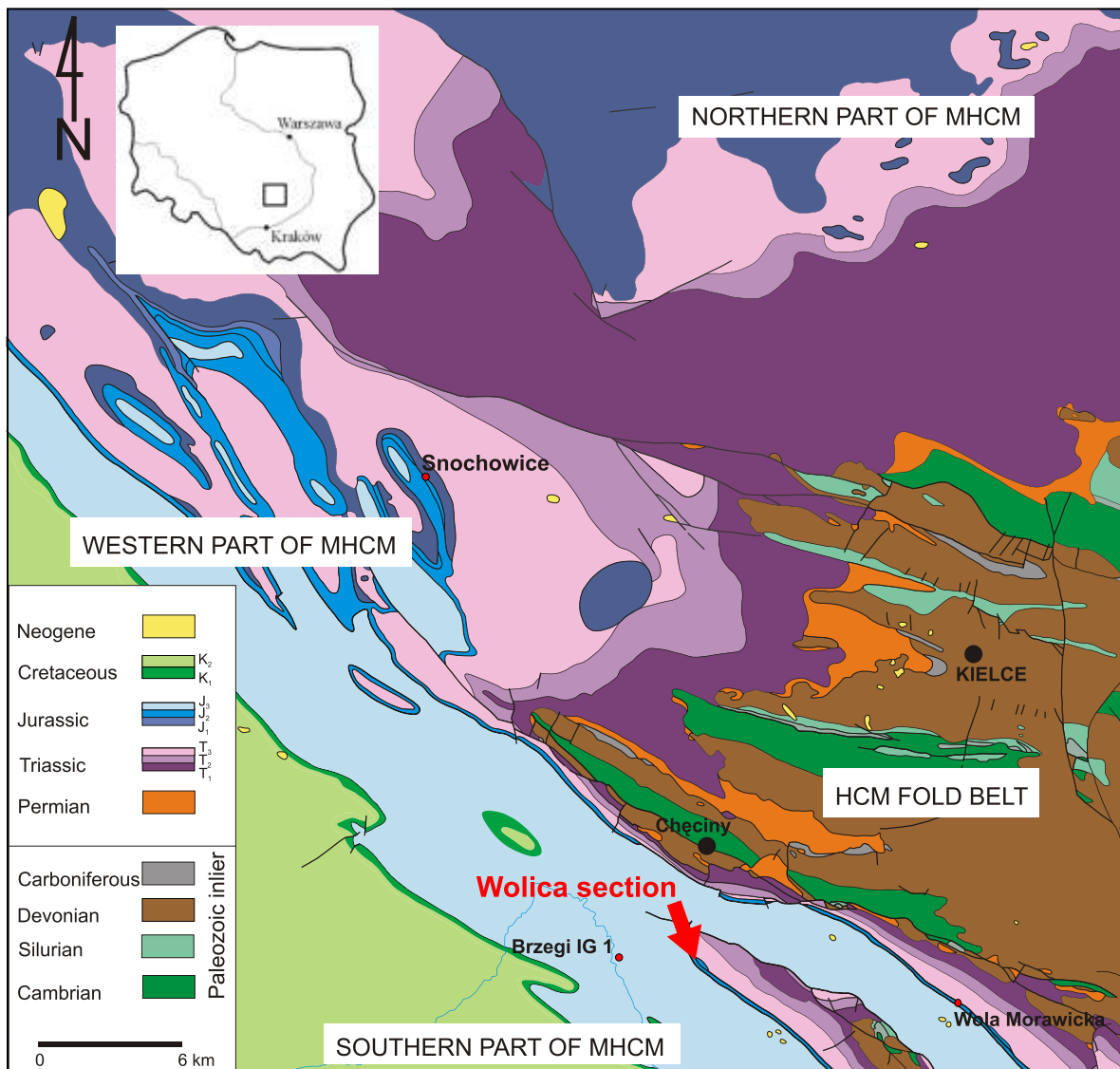


Fig. 1. Geological map of the study area
(compilation after Czarnocki, 1938; Filonowicz 1966, 1976, 1978; Hakenberg, 1973)

HCM Fold Belt – Holy Cross Mountains Fold Belt, MHCM – Mesozoic margin of the Holy Cross Mountains

The post-Variscan relief was entirely buried during the clastic sedimentation of the Buntsandstein. The Buntsandstein is overlain by the Röt and Muschelkalk neritic carbonates (Senkowiczowa, 1970; Trammer, 1975; Szulc, 2000), and siliciclastic and carbonate rocks of the Upper Triassic (Kopik, 1970; Senkowiczowa, 1970). The lower part of the Upper Triassic in the MHCM is represented by various, mainly red and greenish, terrigenous sedimentary rocks (mottled claystones, mudstones and sandstones), with a few intercalations of lacustrine carbonates (limestones, marls, dolomites) and evaporites. Sedimentological aspects of the Keuper are poorly recognized and based on vertical lithological observations performed mainly in the borehole successions. The observed facies associations are interpreted as formed in lacustrine, sabkha and playa environments (Kopik, 1970; Senkowiczowa, 1970; Pawłowska, 1979; Deczkowski and Franczyk, 1988; Gajewska et al., 1997; Fijałkowska-Mader, 2013). The common occurrence of clay-dominated Keuper deposits in an extended area suggests a flat palaeorelief. The Keuper contrasts with the uppermost Triassic sedimentary rocks of lacustrine/fluviial origin, referred to as the Wielichowo Beds, passing upwards into the Zagaje Formation of Rhaetian and Hettangian age (Pie kowski et al., 2014). The succession is represented by grey to greenish sandstones, conglomerates and fine-grained deposits with coal interbeds (Kopik, 1970; Senkowiczowa, 1970; Pawłowska, 1979; Deczkowski, 1997). Due to insufficient Late Triassic biostratigraphic data before the 1980s, informal lithostratigraphic units belonging to the “Keuper” were often mistakenly used as chronostratigraphic units, while some chronostratigraphical units (i.e. Rhaetian) were used in a facies context, which caused much confusion and ambiguities in local stratigraphic terminology. Later, miospore and megaspore palynological studies have allowed for the elaboration of a biostratigraphical framework for the Upper Triassic in Poland and more precise dating of a considerable portion of the succession (Orłowska-Zwoli ska, 1983; Marcinkiewicz and Orłowska-Zwoli ska, 1985, 1994; Marcinkiewicz et al., 2014; Krupnik et al., 2014). As a result, the “Keuper” is assigned a Late Ladinian–Early Rhaetian age, and the lowermost part of the Zagaje Formation has been referred to a Late Rhaetian age (Pie kowski et al., 2008; Pie kowski, 2009).

In the study area, the topmost part of the Upper Triassic succession is generally represented by red coloured fine-grained deposits, which were inconsistently referred to the Keuper (Fig. 2; Lewi ski, 1912; Siemi tkowska, 1967; Hakenberg, 1974) and, in a wrong meaning, to the “Rhaetian” facies (Fig. 2; Jurkiewicz, 1974). The detailed chronostratigraphical age of the succession is still not well-defined. The youngest biostratigraphically dated rocks of the Triassic in the nearby Brzegi IG 1 borehole are attributed to the miospore *Corollina meyeriana* b zone, assigned to the Upper Norian (Fijałkowska-Mader, 2013).

To the south of the HCM Fold Belt, the Upper Triassic strata are overlain with a pronounced disconformity by Middle Jurassic marine black mudstones, which was first noted by Lewi ski (1912) in a railway cutting-section, situated about 2 km to the west of Wolica. Based on lithological similarities to the widely distributed Ore-Bearing Cz stochowa Clay Formation in southern Poland (Kopik, 1998) and the recognized faunal assemblage, a Bathonian (Lewi ski, 1912; Czarnocki, 1927; Siemi tkowska, 1967) or even Bajocian age (Szulczewski, 1967) has been proposed for the unit. The Bathonian age was additionally supported by the finding of the ammonite *Parkinsonia*

sp. in the Wola Morawicka section, documenting the Parkinsoni Zone or the lowermost part of the Zigzag Zone (Filonowicz, 1965), which allowed attribution of the base of these deposits to the Lower Bathonian. Based on assemblages of dinoflagellate cysts, Barski (1999) assigned the mudstones to the Lower and lowermost Middle Bathonian (from the Zigzag Zone to the Progracilis Zone). According to recent biostratigraphical data, the time of the marine transgression in the study area is generally determined as Early Bathonian in age. However, locally the black mudstones are underlain by laterally discontinuous sandstone lithosomes of undetermined age. In the Brzegi IG 1 borehole (4 km to the west of Wolica), a 40 cm thick layer of greenish-grey sandstones occurring below the mudstones, was referred to the Rhaetian by Jurkiewicz (1974), but later a Bajocian age was proposed by Fijałkowska-Mader (2013). Similar greenish-grey sandstones underlying the black claystone succession in the Cz stochowa area were described by Kopik (1998). According to his data supported by ammonite fauna, they were deposited during the latest Early Bajocian age.

Usually, Bathonian black mudstones are overlain by Callovian gaizes and sandy limestones succeeded by an extensive and thick succession of the Upper Jurassic carbonate platform (Matyja, 1977). The Permian-Mesozoic succession is terminated by thick (850 m) Albian-Maastrichtian sedimentary rocks (Cieliski and Paryski, 1970), lying with a pronounced disconformity on the Jurassic. The succession was folded and cut by many faults during Alpine tectonic events (Kutek and Głazek, 1972; Konon, 2007; elaniewicz et al., 2011) and unconformably covered by Miocene strata (Radwanski, 1969, 1973).

MATERIAL AND METHODS

The artificial exposure studied was excavated in 2010 in the rock walls of a quarry road, which cross-cuts the morphological margin of a cuesta located to the south of the village of Wolica (Fig. 3). The road section shows an Upper Triassic (Keuper) to Oxfordian succession, homoclinally dipping to the south (120/18S, dip measurements within 16–22S), structurally representing the southwestern limb of the Zbrza Anticline. The studied interval of the Triassic and Jurassic section (11.5 m thick – see Fig. 4) was tracked laterally over a distance of 200 m. Along the strike, the boundary interval was studied in seven lithologically correlated trenches (1.5–3.5 m thick – see Fig. 5). Lithological (lithology, colour, macrofossils) and sedimentological (grain size, sedimentary structures, character of lithosome contacts) observations were linked with the results of geophysical surveys, performed in order to reconstruct the 3D geometry of the lithosomes occurring in the interval studied.

The lithofacies code applied is compiled on the basis of the Miall (1996) lithofacies code with its modification by Zieli ski (1998); additional symbols are also used for the fine-grained deposits (see Table 1).

The electrical resistivity tomography method (ERT method) was used to recognize the deep-seated geometry and the mutual relationships of the lithosomes (see e.g., Baines et al., 2002; Giocoli et al., 2008; Loke et al., 2013) observed in the walls of the exposure. The assumptions and limitations of the ERT method were described in detail by Kirsch (2009), Loke (2012) and Loke et al. (2013).

The geophysical survey (4 profiles) was performed on an area of 0.6 km² located to the west of the exposure (Fig. 3). The first profile (A–A’), was performed parallel to the western wall of

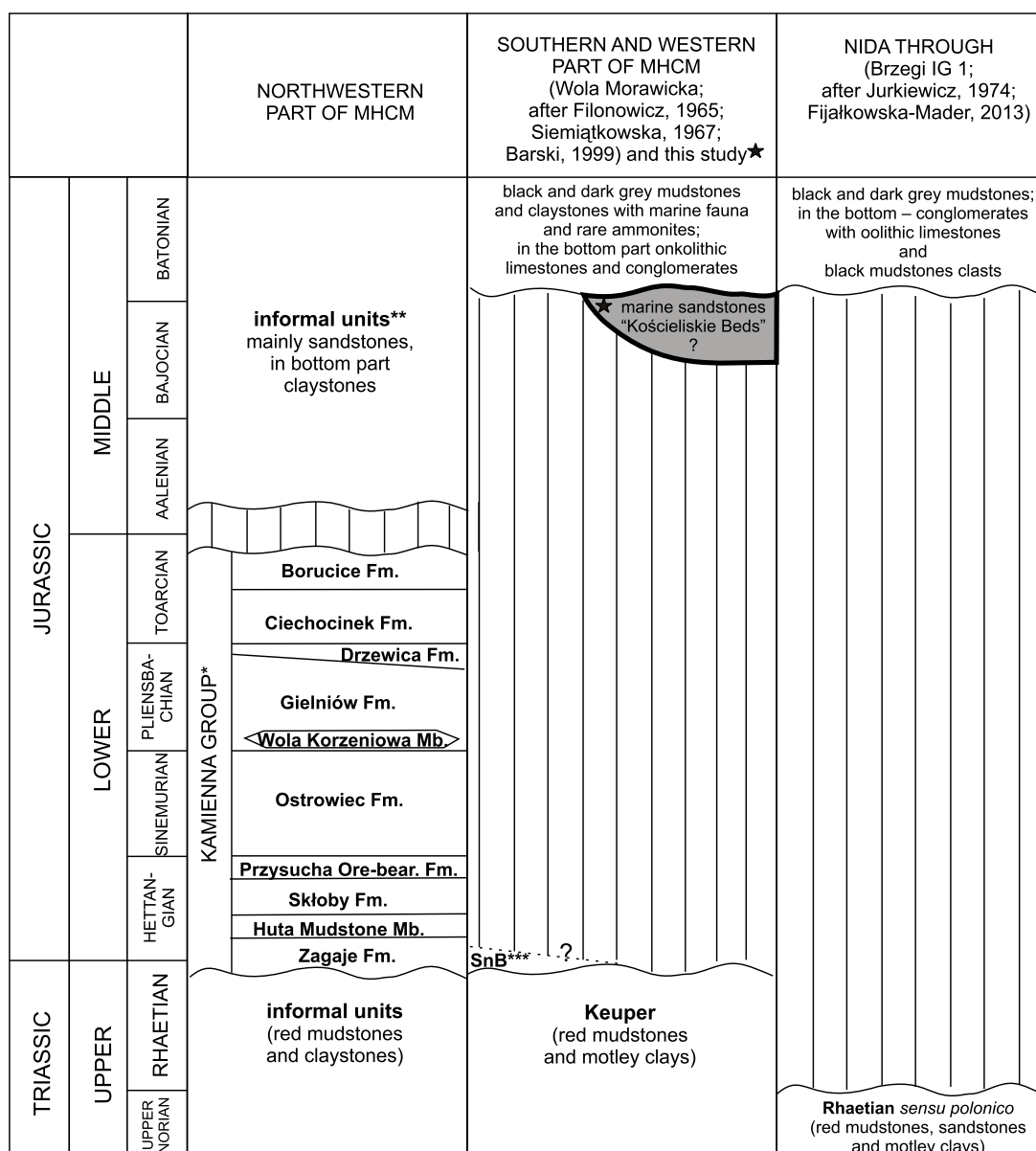


Fig. 2. Lithostratigraphy of the Upper Triassic, Lower and Middle Jurassic in the MHCM

*Kamienna Group – after Piekowski, 2004, simplified; informal units** – after the Stratigraphic Chart of Poland 2008; SnB*** – Snochowice Beds – after Kozłowska, 2012

the exposure and is used to correlate the geophysical survey with the lithology and the lithosome boundaries observed in the exposure. Profiles B–B” and C–C” were located parallel to profile A–A”, 200 and 550 m to the west, respectively; and profile D–D” was made perpendicular to the first three profiles (connecting profiles A–A” and B–B” along the cuesta).

The electrical resistivity survey was conducted using an ABEM 4-channel Terrameter LS. The measurements were taken with a system of 41 to 101 electrodes using the dipole-dipole and gradient configuration. Electrode spacing along the survey profiles was 5 m. The depth range obtained for medium resistivity was from about 50 to 130 m below surface level for the four surveys, depending on the profile length. The obtained horizontal resolution was 5 m, whereas the vertical resolution was 1.5 m in the upper part and 5 m in the lower part of the cross-sections depending on the assumed measurement system.

For the purposes of the biostratigraphical studies (based on dinoflagellate cysts and terrestrial palynomorphs), 22 samples of fresh, non-weathered rocks were collected across the interval studied (see Figs. 4–11 for the “Keuper” and 11 for the overlying rocks). The rock material was digested in 37% HCl and 40% HF acidic solutions following the standard palynological preparation technique (e.g., Poulsen et al., 1998). A residuum of about 50 g per fine-grained rock and about 100 g per sandstone sample was collected for the analysis using a 15 micrometre-diameter sieve and condensed by heavy liquid (2 g/cm³) separation. The prepared slides revealed a few dinoflagellate cysts and terrestrial palynomorphs, and so two or three slides per sample were examined. The palynological analyses of samples with high abundances are based on total counts of 300 dinoflagellate cyst specimens from each slide. Otherwise only qualitative data are provided. Microphotographs were taken using a Nikon Eclipse E-600 microscope equipped with phase contrast and a digital camera.

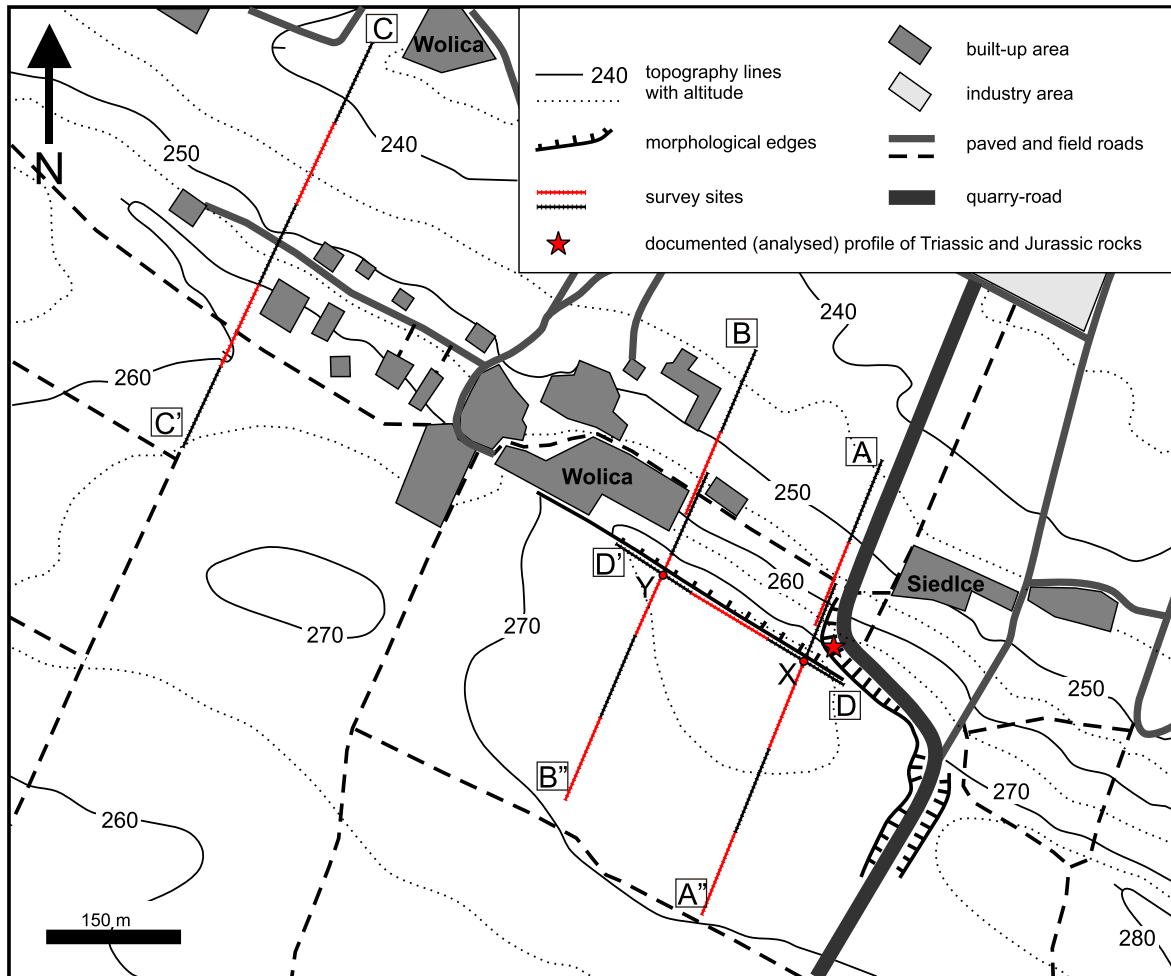


Fig. 3. Location of the geophysical profiles in the Wolica area

LITHOFACIES AND SEDIMENTOLOGY

The studied succession is composed of 14 clastic lithofacies (Table 1).

From the bottom to the top, the lithological succession (Fig. 5) includes several lithological units.

UNIT 1 (4.5 m of thickness visible)

Red-brownish, horizontally bedded mudstones (Mh) occurring at the base of the succession (Fig. 5) are cut by red-brownish fine-grained, horizontally laminated sandstones and siltstones (Sh-Th), fining upwards and with spot occurrences of plant detritus in the lower half. In the top, the siltstones are discoloured and show a massive structure. The next sandstone bed occurring above the erosive surfaces shows planar cross-bedding (Sp; Fig. 6; generally dipping towards the north-west). The sandstones (also discoloured and fine-grained in the top; Ch) are overlain by red-brownish, horizontal and laminated mudstones (Mh) with discoloured, discontinuous laminae and mottled parts with a massive structure [Mm(b)].

UNIT 2a (0.4–0.7 m thick)

The bottom part of Unit 2a is a discontinuous bed (cut by Unit 2b) of yellowish-green mudstones with horizontal lamination (muddy shales; Mh). The bed is lithologically similar to the top part of Unit 1, however, of identical colour as Unit 2b. The base of Unit 2a is very sharp and continuously flat, which suggests its independence from Unit 1.

UNIT 2b (1.7 to 3.5 m; reconstructed maximum thickness in excess of 3.5 m in the central part of the lithosome)

The unit disconformably cuts units 1 and 2a and shows a distinct lens-shaped geometry. The basal part of the lithosome limited to its axial part is composed of yellowish-green, massive, medium-grained sandstones (Sm; Fig. 6C). The succeeding beds are composed of fine-grained, clayey and medium to coarse, well-sorted sandstones. The beds show internal lateral facies changes with coarser and better sorted material in the axial part and finer, silty material on the flanks (Sp-Tr; Fig. 6D).

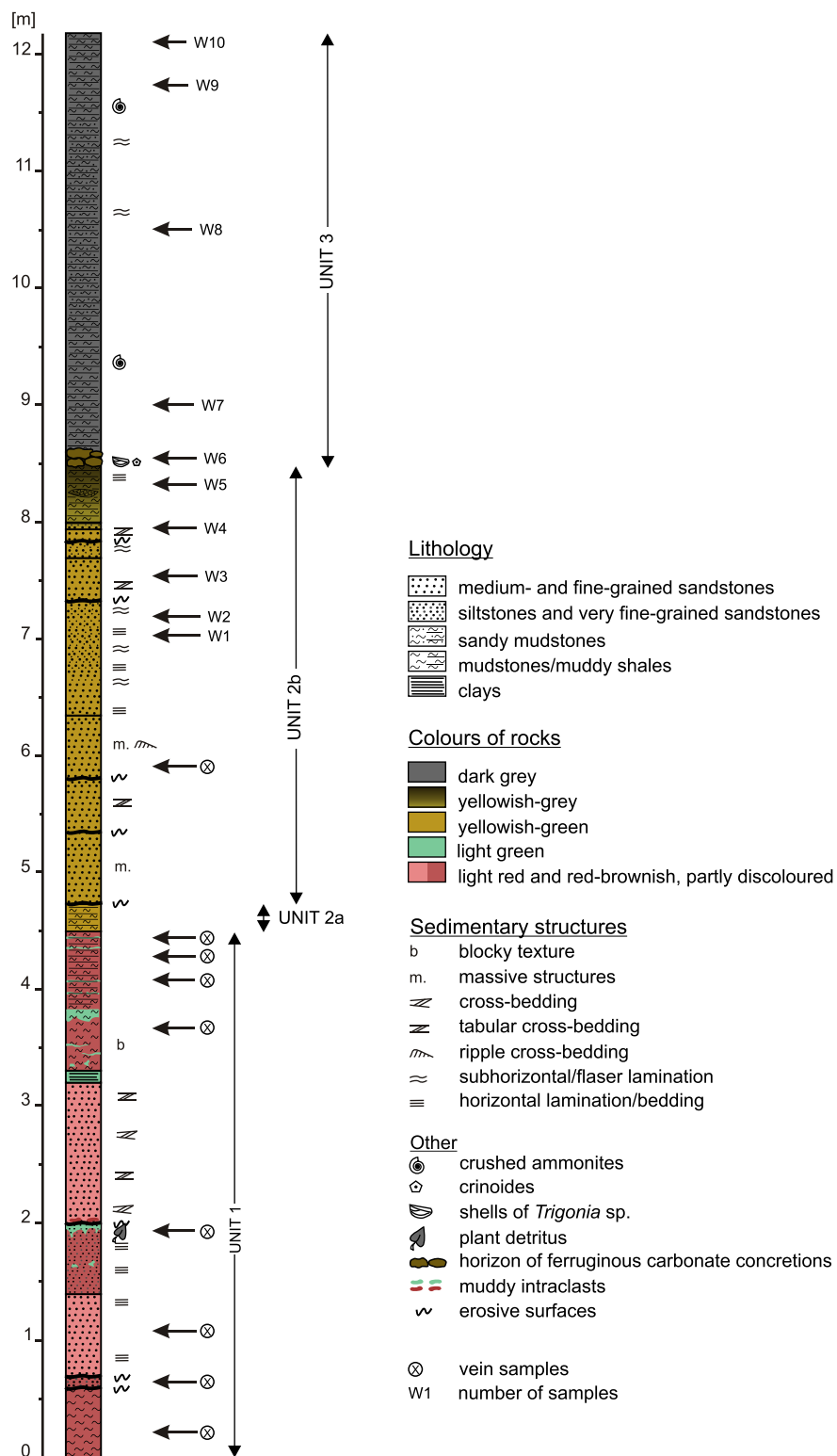


Fig. 4. Lithology and sedimentary structures in the summarized Wolica section

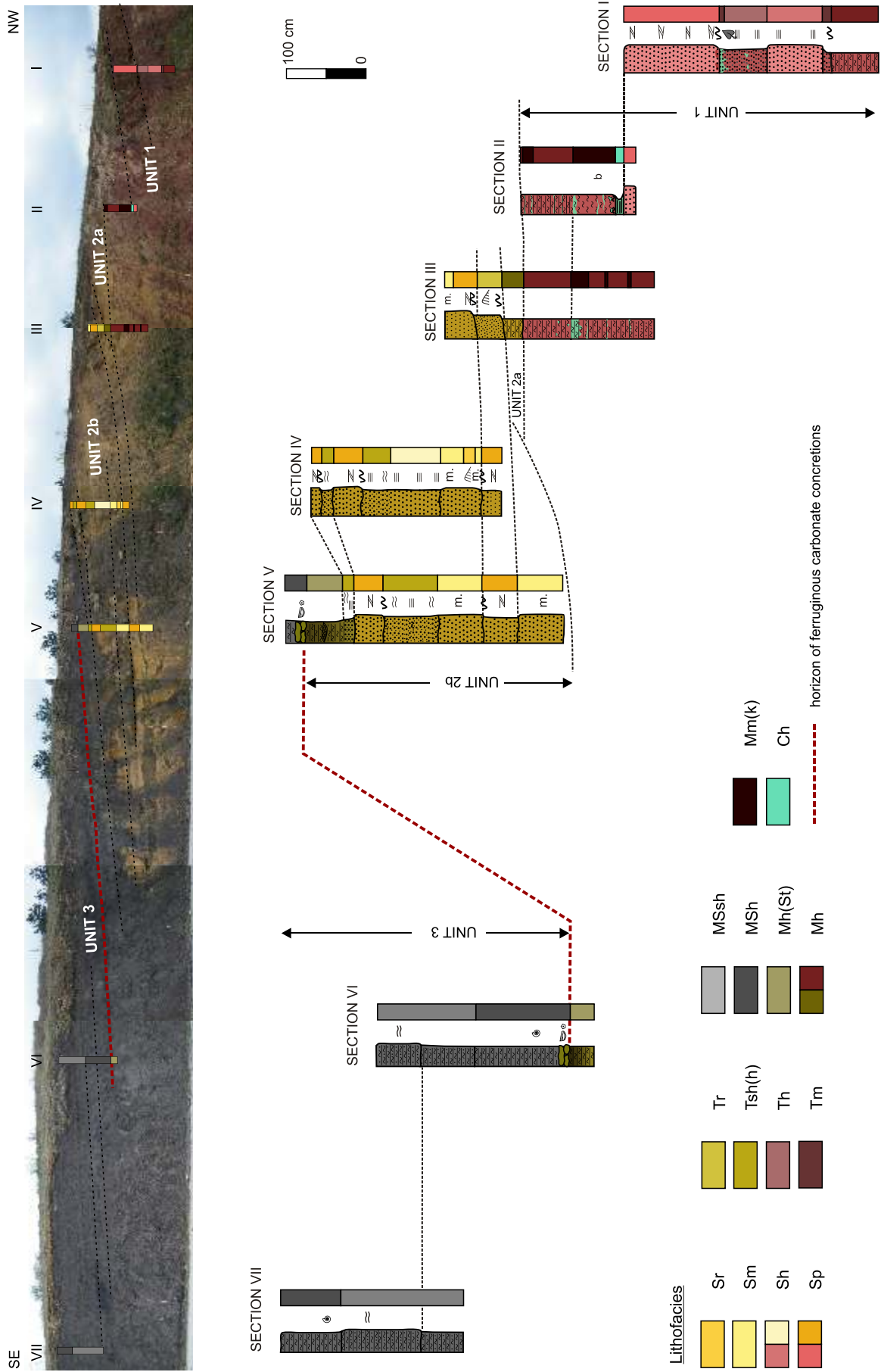


Fig. 5. Lithofacies and units distinguished in the Wolica section

For other explanations see Figure 4

Table 1

Description of lithofacies

Lithology and sedimentary structures	Colour	Content of fossils	Contact	Lithofacies code*
Clays				
Horizontal lamination	light green (probably discoloured)	–	G	Ch
Mudstones				
Massive structure, partially destroyed, blocky texture	reddish-brown; discoloured and discontinuous layers or mottled parts of beds	–	N	Mm(b)
Horizontal to sub-horizontal lamination	reddish-brown or yellowish-green	–	N	Mh
Sub-horizontal lamination; partially sandy; very fine muscovite accumulations	dark grey	–	N	MSsh
Horizontal lamination; horizon of carbonate concretions with stromatolitic structures is observed in the lowermost part; occurrence of sandy laminae	dark grey	rare crushed ammonites and belemnites; algal mats, serpulides, shells of <i>Trigonia</i> sp.	N	MSh
Horizontal lamination, sandy lenses with trough cross-bedding	yellowish-grey and grey	–	G	Mh(St)
Siltstones and very fine-grained sandstones				
Massive structure	reddish-brown	–	E	Tm
Horizontal bedding	reddish-brown; partially discoloured	spot occurrence of plant remains in topmost part	G	Th
Sub-horizontal to horizontal bedding	yellowish-green	–	N	Tsh(h)
Ripple cross-bedding, small scale	yellowish-green or grey	–	G	Tr
Sandstones				
Massive structure; medium-grained sandstones	yellowish-green	–	E	Sm
Horizontal bedding; fine- to medium-grained sandstones	reddish-brown or yellowish-green	–	N	Sh
Planar cross-bedding; medium-grained sandstones; topmost part of yellowish-green sandstones is strongly cemented and contains very fine calcite bioclasts (HCl+)	light red or yellowish-green	–	E	Sp
Ripple cross-bedding; fine-grained sandstones	yellowish-green	–	N	Sr

* Lithology: C – clays, M – mudstones, T – siltstones and very fine-grained sandstones, S – fine- and medium-grained sandstones, MS – sandy mudstones; sedimentary structures: m – massive structure, b – blocky texture, p – planar cross-bedding, r – ripple cross-bedding, sh – sub-horizontal lamination, h – horizontal lamination/bedding; contact of lithofacies with underlying deposits: N – normal, G – gradual, E – erosional

This pattern is underlined by a massive structure or a larger scale of the cross-bedding in the coarser-grained material. The observed cross-bedded laminae consistently dip generally towards the south. The middle part of Unit 2b is dominated by siltstones and very fine-grained sandstones, generally with sub-horizontal and horizontal bedding [Tsh(h)], laterally passing into horizontally bedded sandstones (Sh). The uppermost part of the unit is composed of a sandstone set with planar cross-bedding (Sp) intercalated with siltstones with sub-horizontal bedding [Tsh(h)]. The top bed contains very fine detritus of calcite bioclasts and is overlain by horizontally laminated mudstones with small scale cross-bedded sandy lenses [Mh(St)].

UNIT 3
(in excess of 4.5 m thick)

This unit of black to dark grey mudstones with fully marine fossils contains in its basal part a horizon of ferruginous-carbonate concretions overlying mudstones or sandstones. The discoidal concretions are coated by algal mats, colonized by serpulids and single bivalves attached to the surface (*Trigonia* sp.). The concretions occur in 20 cm thick horizons of a mixed muddy-

-sandy matrix with crinoids and very fine detritus of bivalve shells (MSh with horizon of carbonate concretions; see Fig. 5).

Above the horizon of carbonate concretions black/dark grey muddy shales were noted, horizontally and sub-horizontally laminated, with belemnites and rare, small and crushed fragments of ammonites. They pass gradationally into grey, sandy mudstones with sub-horizontal bedding and very rare, small scale ripple cross-lamination (MSsh). Muscovite accumulations and very fine detritus of calcite bioclasts were observed on the surfaces of the laminae.

The topmost 2 m of Unit 3 are poorly exposed in the exposure. Unit 3 is overlain by Callovian to Lower Oxfordian gaizes (16 m thick), described in detail by [Siemi tkowska-Gi ejewska \(1974\)](#) and [Matyja \(1977\)](#), and succeeded by Oxfordian limestones with a visible thickness of a few metres.

GEOPHYSICAL STUDIES

Direct correlation of profile A–A'' with the exposure wall section, combined with large resistivity contrasts between the rocks forming the Triassic-Jurassic succession in Wolica, allow for the recognition of lithological units on the geophysical profiles.

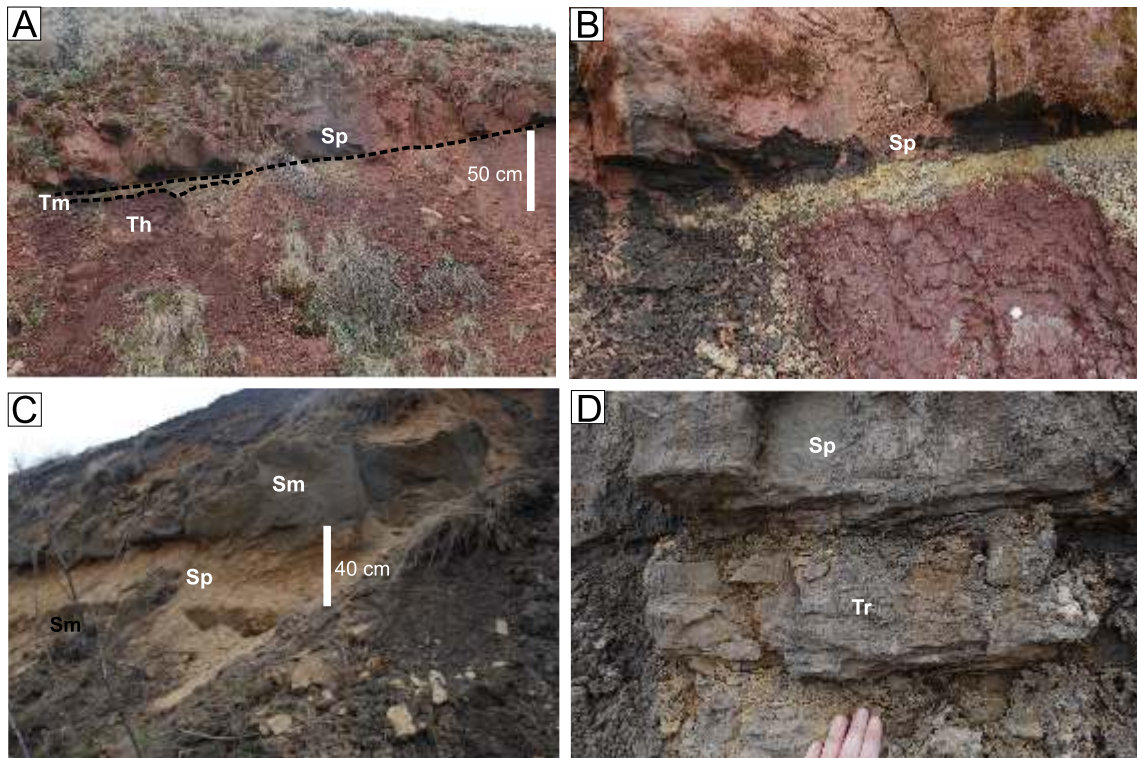


Fig. 6. Lithofacies: A – sandstones with planar cross-bedding on the erosive surface; below siltstones with horizontal bedding (Th); B – below the erosive surface are visible green, massive siltstones (Tm); C – lower part of Unit 2b – massive sandstones cut by sandstones with planar cross-bedding and overlain by massive sandstones; D – upper part of Unit 2b – siltstones with ripple cross-bedding overlain by sandstones with planar cross-bedding

For other explanations see [Table 1](#)

The fine-grained clastics of units 1–3 are characterized by low resistivity (10–50 Ωm) and are visible on profiles A–A', B–B' and C–C' in blue and deep blue colours (Figs. 7–9). The sandstone lithosomes present in this interval contrast strongly with the background in their high resistivity (200–400 Ωm) and are marked on the profiles by red/violet colours (Figs. 7–9). The sandstone lithosomes have irregular thicknesses with a lens-shaped geometry and occur at several levels of the succession (marked as a–f sandy bedforms on the geophysical profiles; Figs. 8 and 9). Based on the geometrical correlation between the exposure wall and the geophysical profiles, lithosomes a–d are assigned to Unit 1, whereas lithosomes e–f are correlated with the sandstone bodies of Unit 2b. The uppermost high resistivity bodies visible on profile B–B' (Fig. 9) are probably located in the basal part of Unit 3. Gaizes and limestones covering Unit 3 are visible as variable, often irregular resistivity distribution in the range of 50 to 400 Ωm . This pattern is probably related to the distribution of karstic processes in the carbonate rocks.

DINOFLAGELLATE CYST ASSEMBLAGES AND AGE INTERPRETATION

A comprehensive palynological study throughout the succession described provides a new stratigraphical interpretation of the sandstones of Unit 2b and refined stratigraphical data for

the black mudstone deposits of Unit 3. Sandy deposits of Unit 2b are characterized by scarce recovery and advanced mechanical destruction of the microfossils. The black mudstone succession of Unit 3 is highly fossiliferous and includes well-preserved marine palynomorphs. The dominant components of the samples are organic dinoflagellate cysts, terrestrial palynomorphs and other land-derived particles with black inertinite and brown wood predominating. Palynological analyses revealed a few dinoflagellate cysts and terrestrial palynomorphs per slide, therefore two or three slides per sample were finally examined.

The stratigraphical ranges of the key dinoflagellate cysts used in the biostratigraphical analysis are based on the synthetic works of [Riding and Thomas \(1992\)](#) and [Poulsen and Riding \(2003\)](#) and on selected papers ([Woollam and Riding, 1983](#); [Prauss, 1989](#); [Feist-Burkhardt, 1994](#); [Stover et al., 1996](#)). The results of the palynological analyses are shown in the range chart (Fig. 10 and Table 2). The age assignment of the samples studied is summarized in Figure 10. Selected marine and terrestrial taxa are photographically documented on the plates (Figs. 11–14).

Samples W1–W3 were collected from pure sandstones (Sp/Sh) of Unit 2b. The low number of the specimens made counting impractical, therefore only qualitative results are presented. All samples yielded dinoflagellate cysts and a few terrestrial palynomorphs (Table 2). Remains of *Ctenidodinium* spp. are the predominant component of all samples, although complete specimens are rare. Beside *Ctenidodinium* spp. and a

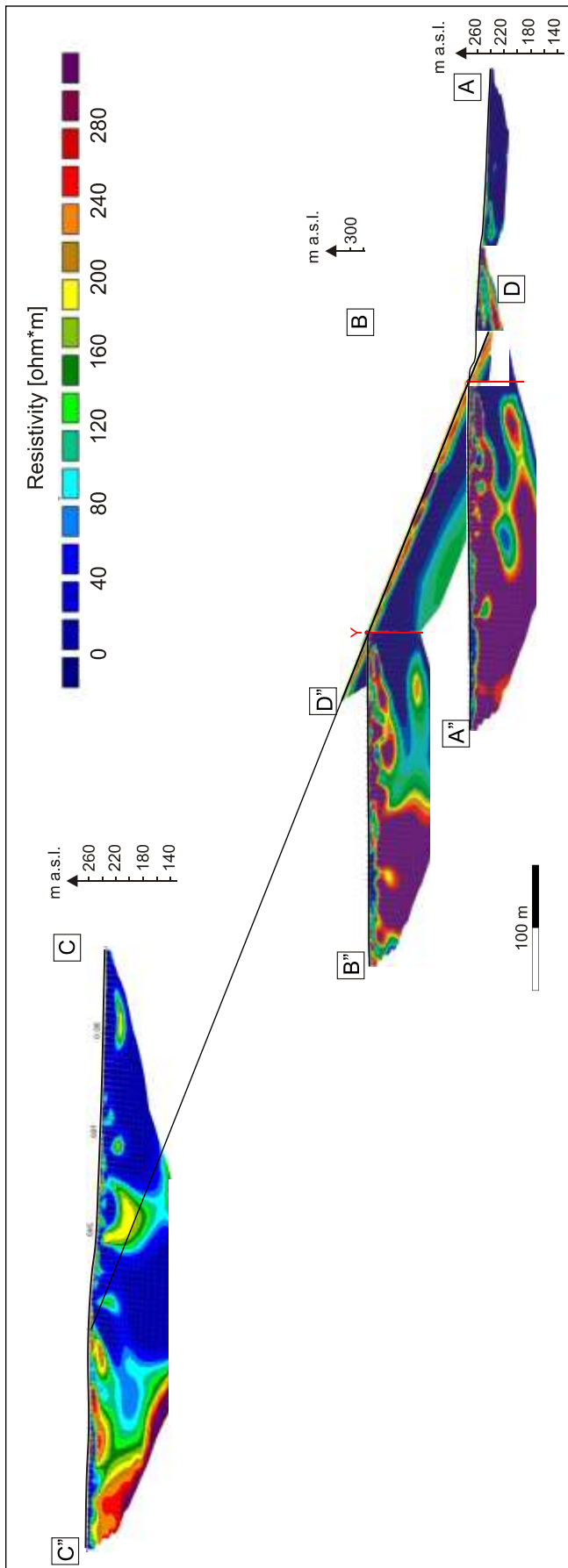


Fig. 7. Geophysical profiles in the Wolica area

few *Sentusidinium* spp., single specimens of *Endoscrinium asymmetricum* and *Pareodinia ceratophora* occur, along with the terrestrially-derived miospores *Callialasporites turbatus*, *Cerebropollenites thierghartii* and *Uvaesporites* sp.

The topmost sample (W4) from the fine-grained sandstones/siltstones with a muddy admixture characterizes a more diversified and better preserved dinoflagellate cyst assemblage with a significant contribution of age-diagnostic taxa. The number of marine microplankton is reduced compared to other organic matter. The latter is dominantly composed of pale grey and light to dark brown, rounded amorphous organic matter and few elongated inertinite particles. A high abundance of green algae, *Botryococcus* sp., is noticeable.

The age assignment of the samples from this interval is based on age-diagnostic taxa according to Riding and Thomas (1992) and Poulsen and Riding (2003). They include *Ctenidodinium combazii*, *Aldorfia aldorfensis*, *Sentusidinium* spp., *Dichadogonyalux selwoodii* and *Lithodinia valensii*. The first appearance of *Ctenidodinium combazii* and *Sentusidinium* spp. in the lowermost sample (W1) indicates an age no older than the Late Bajocian Garantiana Zone. The top of this interval is marked by the last occurrence of *Lithodinia valensii* within the topmost sample (W4) which ranges no younger than the upper boundary of the Bathonian Zigzag Zone.

Samples W5–W7 are located within the black mudstones series of units 2b and 3. Samples W5 and W7 were collected from horizontally laminated mudstones (MSh) and sample W6 comes from carbonate concretions encrusted by microbial mats. Samples W5 and W6 yielded very impoverished palynofloras. The dominant organic matter comprises brown and black woody particles. Organic-walled dinoflagellate cysts are scarce, represented by specimens of *Ctenidodinium* spp. and *Sentusidinium* spp. However, within the impoverished assemblages a few damaged specimens of *Ctenidodinium cornigera* and *C. combazii* were found.

In turn, sample W7 yielded a rich and diverse palynological assemblage. The dinoflagellate cyst association is dominated by *Ctenidodinium* spp. and cysts characterized by apical archeopyles, including *Sentusidinium* spp. and *Kallosphaeridium* sp. Moreover, terrestrial palynomorphs are more diverse than in the previous assemblages. They are represented by bisaccate pollen grains, spores and pollen, brown and black wood and phytoclasts. Additionally, the sample yielded scarce cuticle and prasino-phycean algae.

The dinoflagellate cyst assemblages from this interval indicate the Zigzag Zone of Early Bathonian age. This age assignment is based on the first appearance of *Ctenidodinium cornigera* confined to the lower boundary of this zone and the last occurrence of *Lithodinia valensii*. The extinction of the latter species is assumed to mark the end of the Zigzag Zone according to Riding and Thomas (1992). Nevertheless, it must be mentioned that both taxa co-occur only in sample W7, therefore this constrains the age assignment of the underlying samples (W5 and W6), which yielded only *Ctenidodinium cornigera*. This interval, however, can be slightly wider according to the data provided by Poulsen (1998), since he postulated the FAD of *Ctenidodinium cornigera* at the base of the latest Bajocian Bomfordi Subzone. He also noted an earlier extinction of *Lithodinia valensii* occurring at the base of the Bomfordi Subzone. According to this study, all samples below sample W7 are

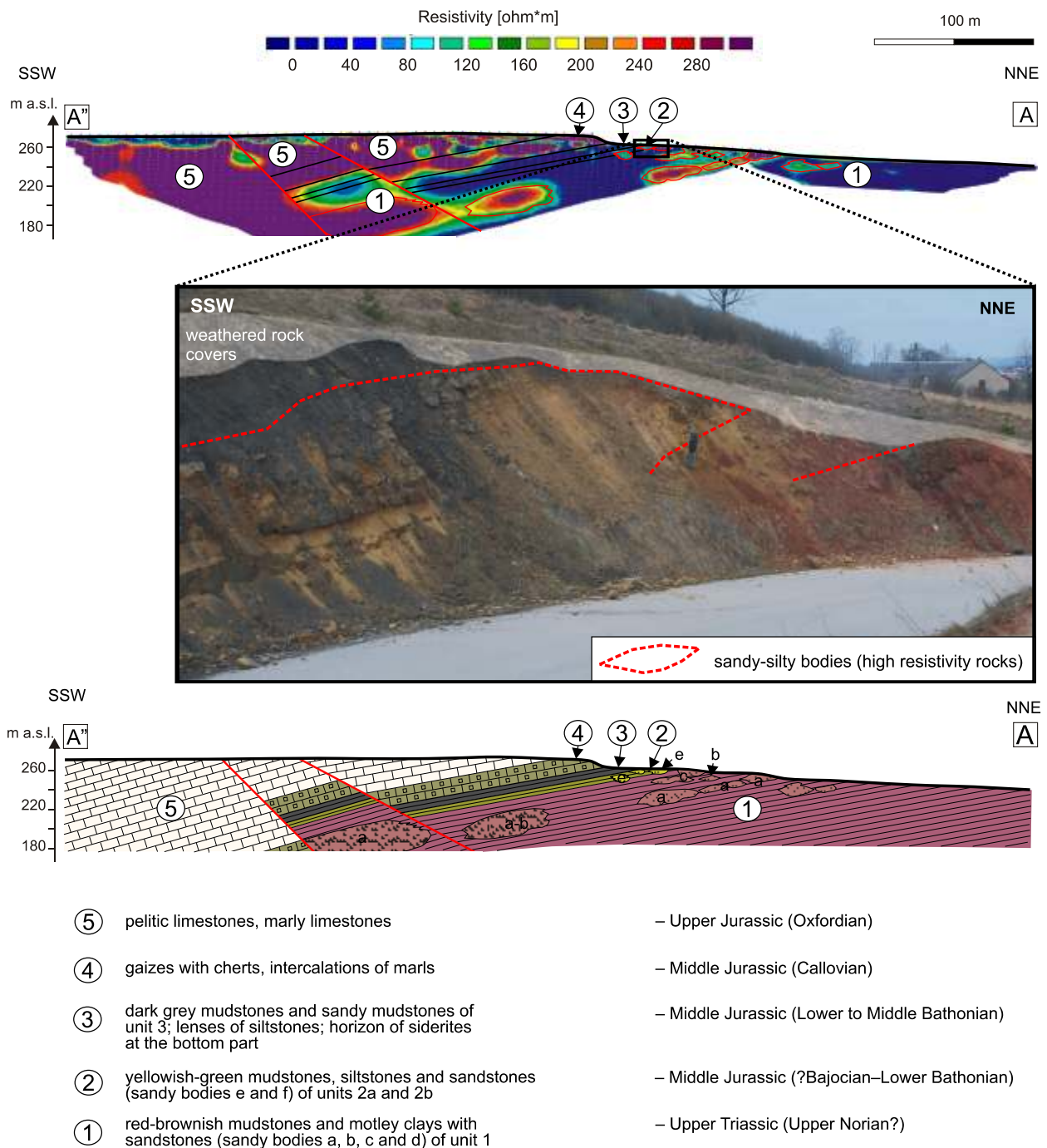


Fig. 8. Geophysical profile A–A'' and geological interpretation (photo by B.A. Matyja)

probably not younger than the Bromfordi Subzone. This interpretation, however, must be regarded as tentative due to restricted data availability.

Sample W8 was collected from the middle part of the black mudstones succession. The palynological content of this sample is relatively rich and taxonomically moderately diverse. The consistent dominance of *Ctenidodinium* spp., *Aldorfia* spp. and *Sentusidinium* spp. is typical of the Bathonian. Moreover, a higher abundance of *Nannoceratopsis* spp. was observed. The recovery of terrestrial palynomorphs is again very rich. A few specimens of *Botryococcus* sp. and cuticle fragments were observed.

The sample is assigned to the Tenuiplicatus Zone due to the presence of two key species *Atopodinium polygonale* and *Atopo-*

dinium prostatum. Riding and Thomas (1992) correlate the FAD of *Atopodinium prostatum* and the LOD of *Atopodinium polygonale* with the lower and upper boundary of the Tenuiplicatus Zone, respectively. The LOD of the latter species is correlated by Poulsen (1998) with the upper boundary of the Progracilis Zone, therefore an expanded interval can also be considered.

Samples W9 and W10 come from the topmost part of the black mudstones succession available for study. Both samples are taxonomically most diverse, however, they reveal an evident predominance of *Ctenidodinium* spp. The terrestrial components of the samples are also abundant and well-preserved. This observation refers especially to the topmost sample W10, which is dominated by large terrestrial particles including cuticle, and brown and black wood. Large amounts of wood are unbroken,

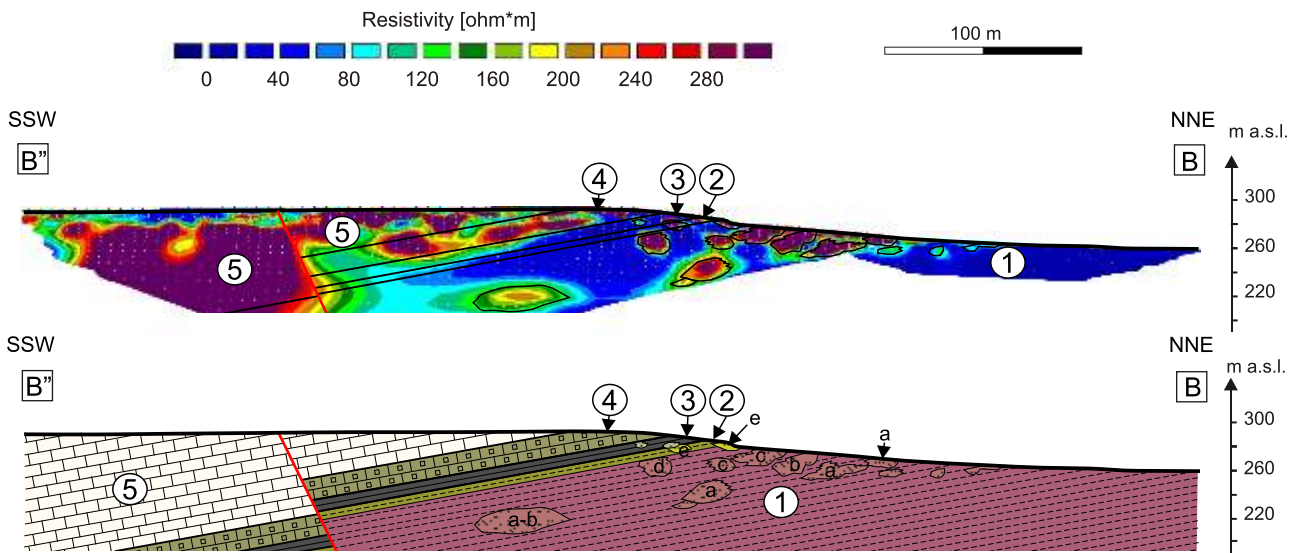


Fig. 9. Geophysical profile B-B'' and geological interpretation

For explanations see Figure 8

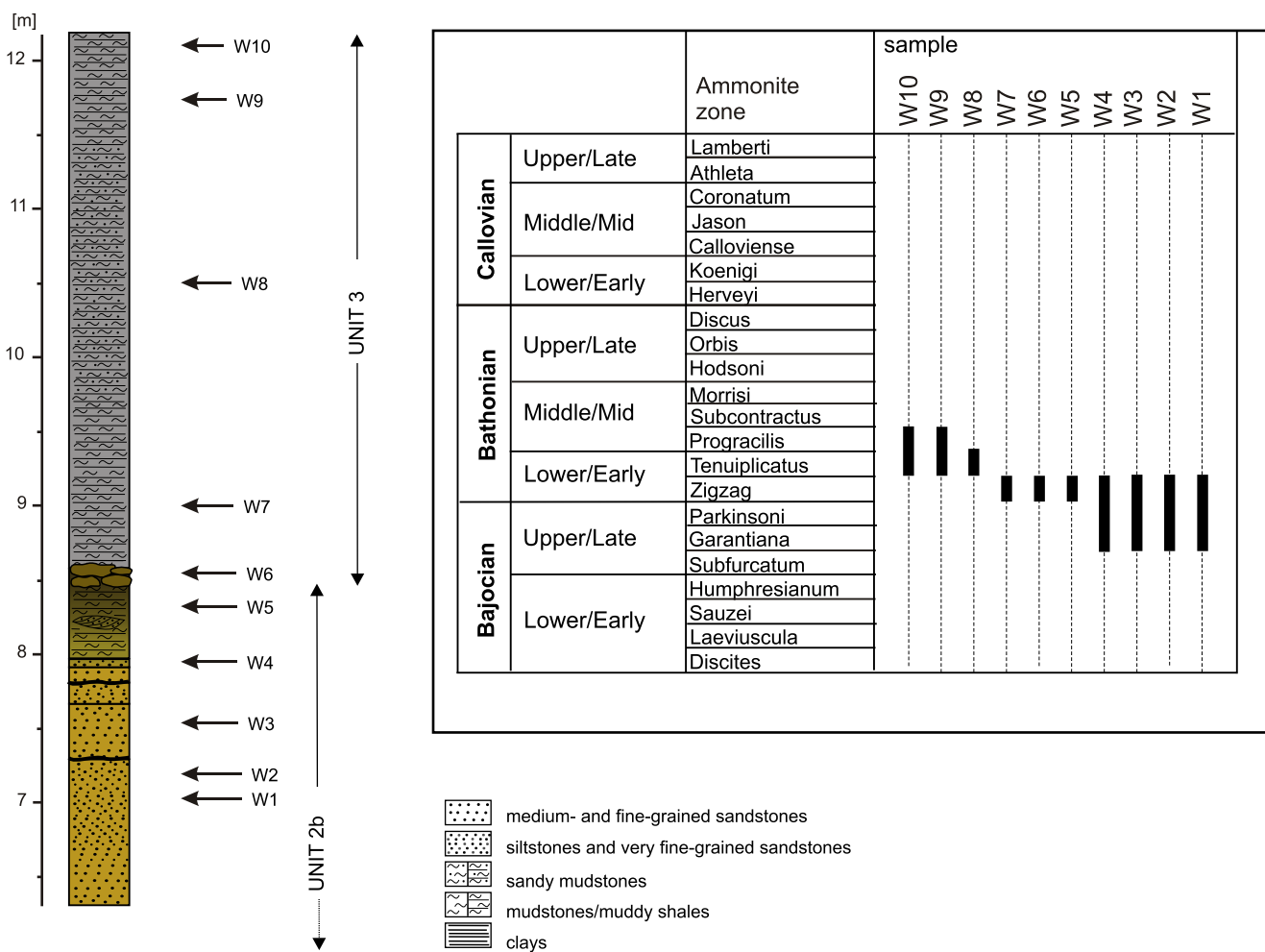


Fig. 10. Stratigraphy of the Wolica section

For explanations see Figure 4

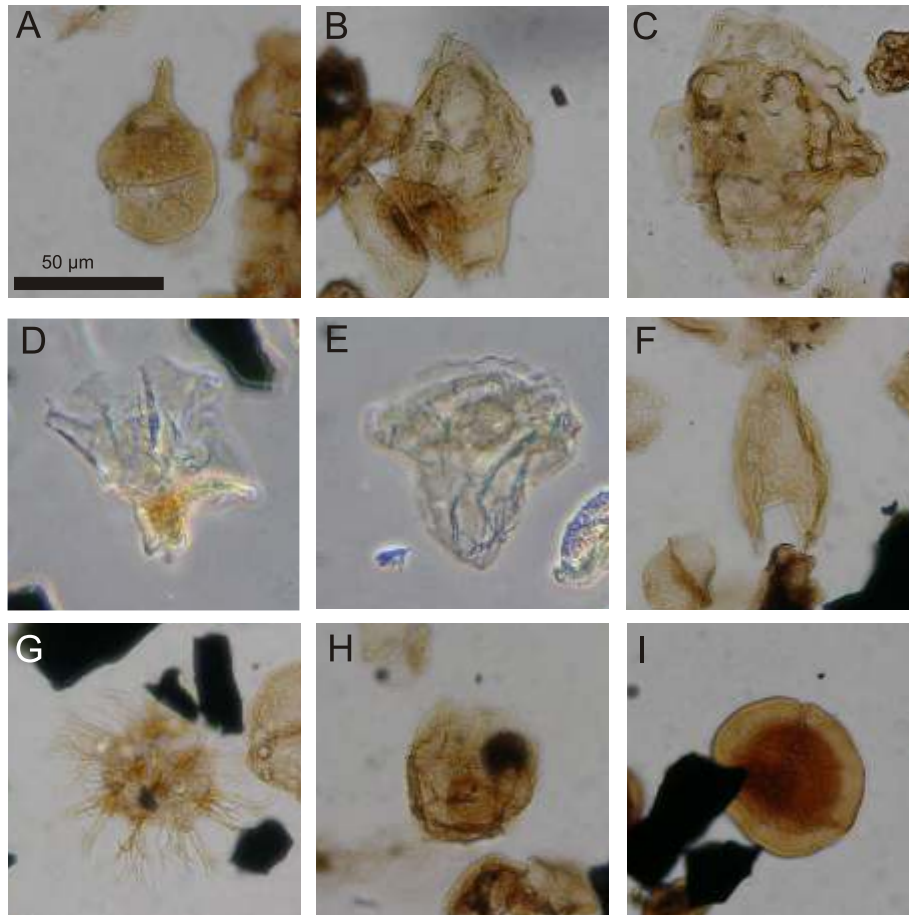


Fig. 11. Selected palynomorphs from Wolica section (50 micrometres scale bar)

A – *Pareodinia ceratophora* Deflandre, 1947, sample W7; **B** – *Tubotuberella apatela* (Cookson and Eisenack, 1960) Ioannides et al., 1977, sample W9; **C** – *Endoscrinium asymmetricum* Riding, 1987, sample W10; **D** – *Atopodinium polygonale* (Beju, 1983) Masure, 1991, sample W9; **E** – *Eodinia poulsenii* Barski, 2002, sample W5; **F** – *Nannoceratopsis spiculata* Stover, 1966, sample W7; **G** – *Surculosphaeridium? vestitum* (Deflandre, 1939) Davey et al., 1966, sample W10; **H** – *Meiourogonyaulax caytonensis* (Sarjeant, 1959) Sarjeant, 1969, sample W4; **I** – *Callialasporites dampieri* (Balme, 1957) Dev 1961, sample W8

lath- and needle-shaped. Some subsidiary land-derived particles have also been encountered. They include cortex, resin and a remarkable amount of spores and pollen grains.

According to the key dinoflagellate cysts, the age of samples W9 and W10 is attributed to the *Tenuiplicatus-Progracilis* zones interval. It is based on the FAD of *Atopodinium prostaticum* and the LOD of *Carpathodinium predae* (Riding and Thomas, 1992) limiting this time interval.

DEVELOPMENT OF SEDIMENTATION

UNIT 1

The red/mottled colours of Unit 1 (?Upper Norian) suggest deposition in continental environments and semi-arid or arid climate conditions.

The finer-grained sedimentary rocks of Unit 1 may be referred to aquatic conditions with a low energy of hydraulic transport or deposition from suspension. Horizontally laminated mudstones (Mh) and the overlying, laterally continuous, fining-upwards sandy-silty deposits with rare plant detritus, mainly

with horizontal bedding (Tm-Sh-Th-Tm succession), probably represent proximal floodplain deposits and sheet-flow deposits. They were formed when flow occurred during flood stages on the floodplain area. Similar, fine-grained, laminated silty-muddy deposits are usually interpreted as a floodplain succession by many authors (Miall, 1996; Love and Williams, 2000). Upper Permian, horizontally laminated red mudstones cropping out in the Vyazovka Ravine in the Ural Mts., similar to lithofacies Mh presented herein, were interpreted by Newell et al. (1999) as the effect of suspended sediment deposition from shallow floodwaters on the proximal parts of floodplains.

The presence of cross- and horizontal-bedded, coarser-grained sandy-silty deposits of Unit 1 indicates hydraulic transport. Based on the relations and geometry of the lithosomes, observed in the exposure and revealed by the geophysical survey (see Figs. 9 and 10), the sandstone bodies are interpreted as fluvial channel-fills incising proximal floodplain sediments (compare with e.g., Miall, 1996). Similar, cross- and horizontal-bedded sandy-silty deposits a few metres thick scattered among the red, laminated mudstones succession from the Upper Triassic red clastic succession of southwestern Germany are interpreted as channel-fills and lateral accretionary bedforms by Hornung and Aigner (1999). Newell et al. (1999) have

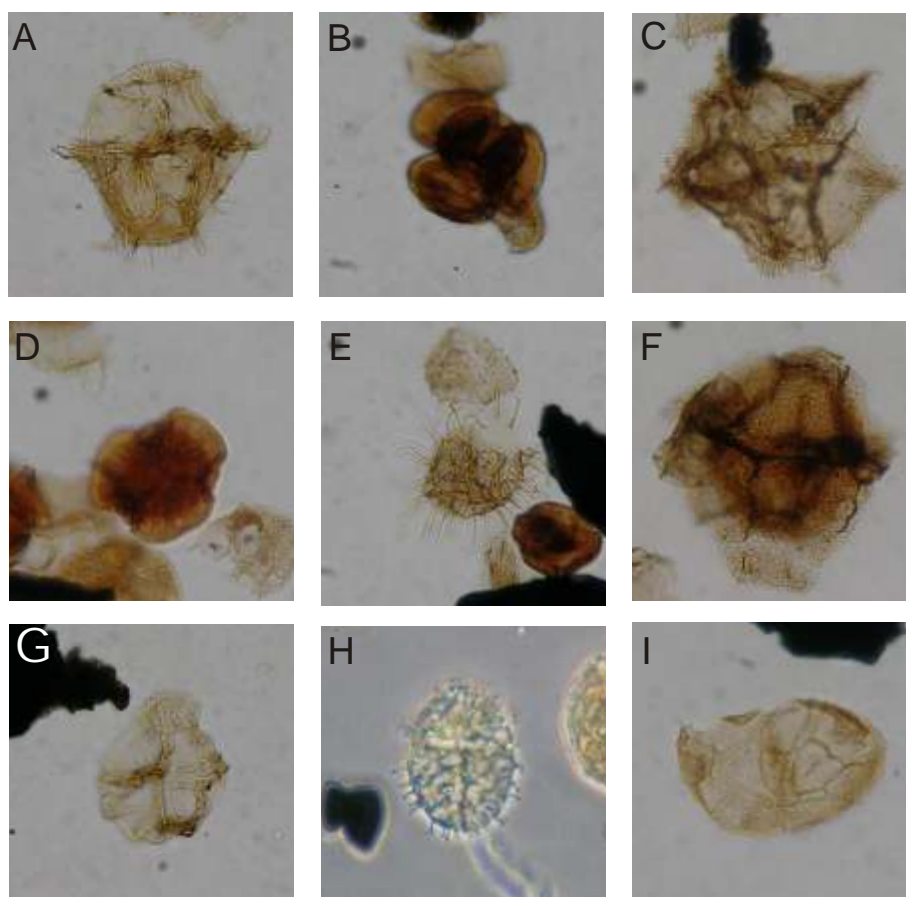


Fig. 12. Selected palynomorphs from Wolica section (50 micrometres scale bar)

A – *Ctenidodinium cornigerum* (Valensi, 1953) Jan du Chêne et al., 1985, sample W7; **B** – *Classopolis* sp. (tetrad), sample W5; **C** – *Rhynchodiniopsis? regalis* (Gocht, 1970) Jan du Chêne et al., 1985, sample W4; **D** – *Callialasporites trilobatus* (Balme 1957) Dev 1961, sample W7; **E** – *Impletosphaeridium ehrenbergii* (Deflandre, 1947) Islam, 1993, sample W9; **F** – *Lithodinia valensii* (Sarjeant, 1966) Gocht, 1976, sample W7; **G** – *Atopodinium prostaticum* (Drugg, 1978) Masure, 1991, sample W9; **H** – *Epiplosphaera gochtii* (Fensome, 1979) Brenner, 1988, sample W4; **I** – *Durotrigia* sp., sample W7

interpreted sandy lenses in red mudstones successions as channel-fills of a distributary stream system, developed on mudflats on an alluvial plain. The cross-bedded sandstones (Sp; Fig. 6B) were probably formed during lateral accretion of point bars. The light green clays at the top of lithofacies Sp document weathering processes on the emergent point bar surface after channel avulsion. The uppermost, red, partially discoloured mudstone succession [Mm(b)-Mh] of Unit 1 were formed on a floodplain.

The characteristic irregular, mottled part of the rocks and the blocky texture of the mudstones are the main indicators of weathering processes and seasonal wetting and drying events. Increase in groundwater level during floods could have turned the flat floodplain even into a temporary lake. During the drying events, the red muddy deposits shrunk and a blocky texture was formed. These processes are frequently described from continental red beds (Newell et al., 1999; Love and Williams, 2000). The hot, semi-arid and arid conditions of sedimentation were suggested also by Fijałkowska-Mader (2013, 2015) for similar Upper Triassic red clastic successions in the Brzegi IG 1 borehole based on palynomorph spectra.

The spatial arrangement of the sandy channels within Unit 1 showing the lateral range of the depositional zone, depth of ero-

sion, and channel avulsion (see sandy bedforms a, b, c and d in Figs. 9 and 10) is well-visible on the ERT profiles. Modern channel systems and the effect of avulsion processes in clastic, especially fluvial/alluvial environments have been commonly successfully detected by the application of ERT methods (Baines et al., 2002; Giocoli et al., 2008; Loke et al., 2013; Kasprzak and Traczyk, 2014). The particular sandy bedforms are over 20 m thick and generally less than 50 m wide. The orientation of the palaeovalley axis is close to WNW, generally similarly to the NW dip of the planar cross-bedded sandy sets; hence the local palaeoflow of rivers was to the north-west.

UNIT 2a

The rapid horizontal colour change between Unit 1 and the 40 cm thick, yellowish-green mudstones of Unit 2a suggests a radical change of the sedimentary regime. The mudstones represent suspension-laid deposits of unknown age, formed during the Late Norian to the late Bajocian interval time. It is possible that the bed represents an early stage of the Bajocian-Bathonian transgression, however, its origin via an independent sedimentary episode cannot be excluded.

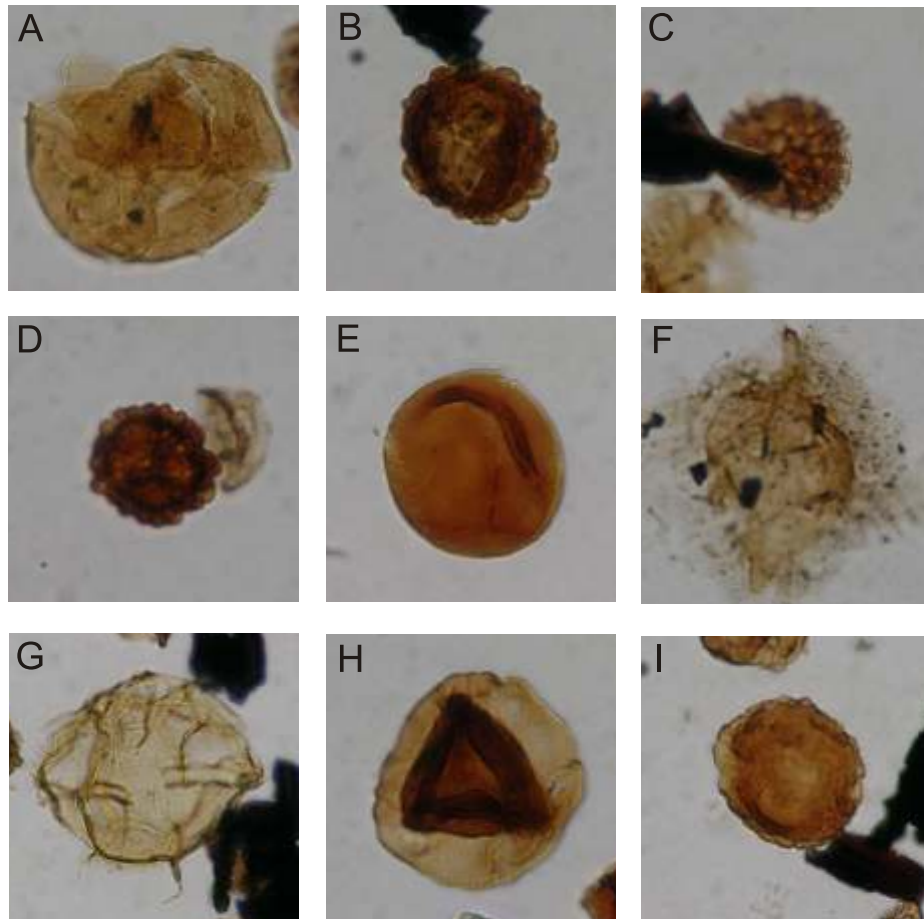


**Fig. 13. Selected palynomorphs from Wolica section
(50 micrometres scale bar)**

A – *Korystocysta gochtii* (Sarjeant, 1976) Woollam, 1983, sample W10; **B** – *Cerebropollenites mesozoicus* (Couper) Nilsson 1968, sample W8; **C** – *Lycopodiumsporites* sp. sample W9; **D** – *Uvaesporites* sp., sample W2; **E** – *Todisporites* sp., sample W9; **F** – *Kalyptea stegasta* (Sarjeant, 1961) Wiggins, 1975, sample W9; **G** – *Dichadogonyaulax sellwoodii* Sarjeant, 1975, sample 4; **H** – *Callialasporites turbatus* (Balme) Schulz, 1967, sample W3; **I** – *Callialasporites microvelatus* Schulz, 1966, sample W7

UNIT 2b
(?Upper Bajocian–Lower Bathonian)

The pronounced erosive surface below Unit 2b and its distinct lithofacies content suggests a distinctive sedimentary event responsible for the formation of the succession. The shape of the bottom surface is consistent with a relatively flat palaeovalley. Geophysical data indicates the uniqueness of the form visible in the exposure, without any counterparts in the area studied (0.6 km²).

Sandy-silty lithofacies with planar cross- to horizontal-bedding (Sp and Sh) are the effect of hydraulic, channelized and preferentially unidirectional transport of the sandy material to the south. The facies resemble fluvial channel-fills in deltaic environments with a rising level of the erosive base – such as cross-bedded sandstone facies, known from the Holocene deltaic successions of the Mississippi (Penland et al., 1988). Similar facies assemblages are also typical of channel-fills, formed in the inner, landward part of estuaries, where river processes dominate (e.g., Leckie and Singh, 1991). The latter option may be supported by the increase of marine influence observed towards the top of the section, confirmed by the occur-

rence of characteristic, freshwater algae – *Botryococcus* sp. (see Guy-Ohlson, 1992) and terrestrial components such as *Callialasporites turbatus*, *Cerebropollenites thiergartii* and *Uvaesporites* sp. with an increasing admixture of marine plankton (dinoflagellates). The horizontally or sub-horizontally-bedded siltstones and very fine grained sandstones [Tsh(h)], present in the upper part of the lithosome, may be assigned to estuarine mouth bars, probably re-distributed by wave agitation. The topmost part of the unit composed of yellowish-grey mudstones with small-scale, trough cross-bedded sandy lenses [Mh(St)] is interpreted as an outer estuarine zone or prodelta mud deposits formed during successive pulses of transgression and sea level rise.

The generally fining-upward trend of Unit 2b represents transgressive deposits infilling a minor palaeovalley by a succession deposited in river-mouth conditions. The main trigger of the deposition was probably a rise of the erosive base, which allowed rapid aggradation of the sediment pile. However, the observed sedimentary record indicates that the rate of sea level rise clearly surpassed the delivery of the clastic material by the river (see Dalrymple and Choi, 2007), hence indicating the small scale of the river. This type of estuarine-like environment

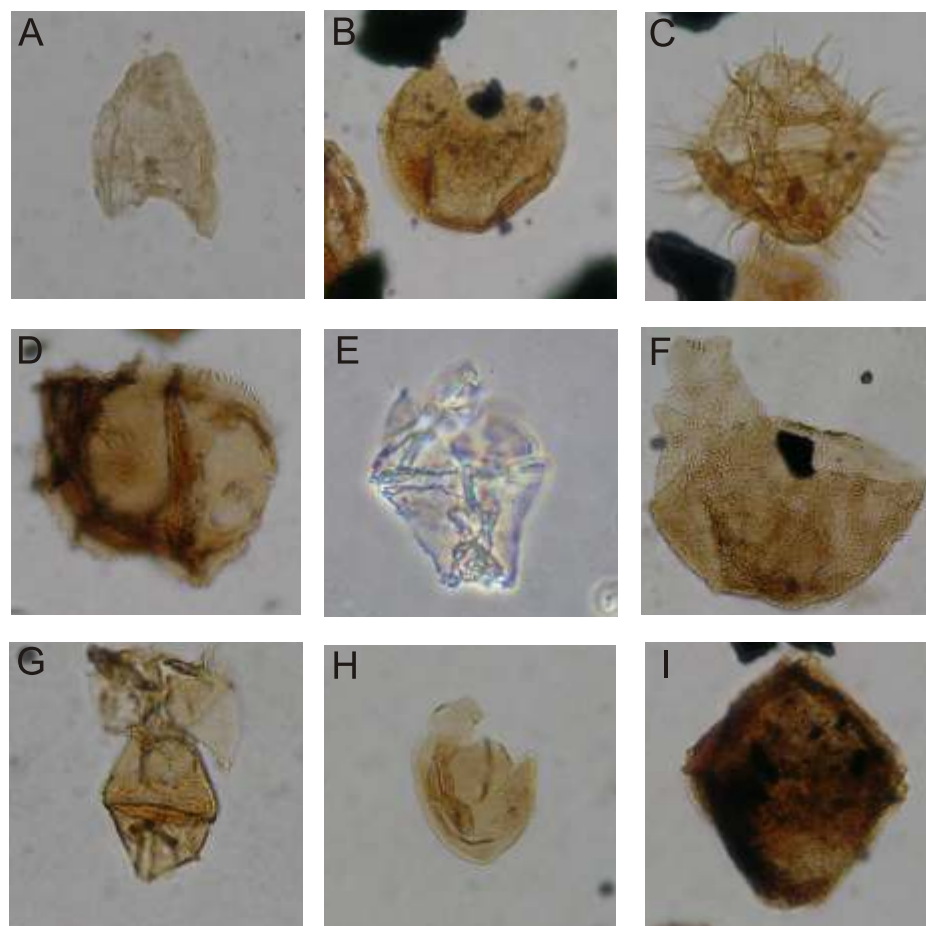


Fig. 14. Selected palynomorphs from Wolica section

A – *Nannoceratopsis gracilis* Alberti, 1961, sample W8; **B** – *Meiourogonyaulax cristulata* (Sarjeant, 1959) Sarjeant, 1969, sample W9; **C** – *Ctenidodinium cornigerum* (Valensi, 1953) Jan du Chêne et al., 1985, sample W7; **D** – *Ctenidodinium continuum* Gocht, 1970, sample W8; **E** – *Atopodinium prostaticum* (Beju, 1983) Masure, 1991, sample W10; **F** – *Dissiliodinium willei* Bailey and Partington, 1991, sample W7; **G** – *Carpathodinium predae* (Beju, 1971) Drugg, 1978, sample W10; **H** – *Kallosphaeridium praussii* Lentin and Williams, 1993, sample W8; **I** – *Aldorfia aldorfensis* (Gocht, 1970b) Stover and Evitt, 1978, sample W7

may be dominated by riverine processes, hence sedimentary structures and ichnofossils typical of tides (e.g., herringbone stratification) may be absent (Roswsetti and Netto, 2006; Dalrymple and Choi, 2007). The timing of the Middle Jurassic transgression in the Wolica area, based on the biostratigraphical data provided, may be estimated at the Bajocian-Bathonian transition.

UNIT 3
(Lower Bathonian–lowermost Middle Bathonian)

This unit was formed in open marine conditions probably during further sea level rise. The sedimentary features are typical of the mudstone lithofacies of the Upper Bajocian-Bathonian Ore-Bearing Cz stochowa Clay Formation, described in detail from the southernmost part of the Polish Basin (Leonowicz, 2013). According to the model, mudstones with indistinct parallel lamination of this formation may be interpreted as deposited from suspension in the marginal part of a shallow epicontinental sea, below storm wave base. Supply

of very fine detritus of calcite shells, muscovite and silty-sandy quartz grains in the upper part of Unit 3 was probably associated with seaward migration of the prodelta or, as in the Cz stochowa area, with deposition from fine-grained suspension currents and current reworking of sea-floor sediments during storm episodes. The occurrence of a horizon of ferruginous, carbonate concretions with coatings of algal mats and encrustations of bivalves and *Trigonia* sp. in the bottom part of Unit 3 suggest shallow marine, periodically high-energy, littoral sedimentary conditions. Similar concretions of oncolite-type were reported by Siemi tkowska-Gi ejewska (1970) from the Bathonian mudstone succession cropping out in the railway cutting near Wolica, and by Szulczewski (1967) from the Bathonian deposits in the Wola Morawicka section. Szulczewski (1967) interpreted these as stromatolitic structures formed in shallow marine, probably littoral conditions. A high content of iron compounds could have resulted from the decay of organic matter transported by the river to the marine embayment. Additional bio-encrustations enhance their resemblance to hiatus concretions from the Middle Jurassic Ore-Bearing Cz stochowa Clay Formation from the southern-

Table 2

Distribution of dinoflagellate cysts and other palynomorphs in Wolica section

Sample	W1	W9	W8	W7	W6	W5	W4	W3	W2	W1
<i>Adnatosphaeridium caulleryi</i>			12							
<i>Aldorfia aldorfensis</i>			20	36			27			
<i>Atopodinium polygonale</i>		8								
<i>Atopodinium prostaticum</i>	10	4								
<i>Atopodinium</i> sp.	3	5								
<i>Botrycoccus</i> sp.			X				XXX			
<i>Callialasporites microvelatus</i>	X	X	X	X	X				X	
<i>Callialasporites trilobatus</i>		X	X							
<i>Callialasporites turbatus</i>	X		X	X		X		X		X
<i>Carpathodinium predae</i>	12	9								
<i>Cerebropollenites macroverrucosus</i>		X		X						
<i>Cerebropollenites mesozoicus</i>	X	X	X							
<i>Cerebropollenites thiergharti</i>			X			X	X			X
<i>Classopolis</i> sp.		X				X				
<i>Ctenidodinium combazii</i>	133	115	119	99	20	12	104	11	8	15
<i>Ctenidodinium cornigerum</i>	23	34	19	41	3	5				
<i>Ctenidodinium continuum</i>	11	5	21				25			
<i>Ctenidodinium</i> sp.	1				7	5				
<i>Dichadogonyalux selwoodii</i>	3	12	7				23		4	
<i>Dissiliodinium willei</i>	4	2	7	8			5			
<i>Durotrigia</i> sp.	6	3	9	12						
<i>Ellipsoidictyum cinctum</i>	2		1							
<i>Endoscrinium asymmetricum</i>	3	6	7					2	1	
<i>Eodinia poulsenii</i>	11	8	8	17		4				
<i>Epiplosphaera gochtii</i>	5	12					19		2	
<i>Escharisphaeridia granulata</i>	6		7			4				
<i>Gonyaulacysta jurassica adecta</i>							5			
<i>Implethosphaeridium ehrenbergii</i>	2	6								
<i>Ischyosporites variegates</i>		X								
<i>Kallosphaeridium praussi</i>	6	7	3			6	11			
<i>Kalyptea stegasta</i>	2	10	3				4			
<i>Korystocysta gochtii</i>	17	12	15	12			15			
<i>Korystocysta pachyderma</i>	4	7		3						
<i>Leptolepidites major</i>		X				X				
<i>Lithodinia valensii</i>				6			2			
<i>Lycopodiumsporites</i> sp.		X								
<i>Meiourogonyalux caytonensis</i>				4			5			
<i>Meiourogonyalux cristulata</i>	1	2								
<i>Nannoceratopsis gracilis</i>			15				6			
<i>Nannoceratopsis spiculata</i>		7		21			22			
<i>Pareodinia ceratophora</i>	23	14	12	19		5	23		3	2
<i>Rhynchodiniopsis regalis</i>			6	8			6			
<i>Sentusidinium</i> sp.	9	4	4	14		12		2	1	3
<i>Surculosphaeridium? vestitum</i>	3	5								
<i>Todisporites</i> sp.		X	X							
<i>Tubotuberella apatela</i>		3	5							
<i>Uvaesporites</i> sp.	X		X						X	

X – present, XXX – abundant

most part of the Polish Middle Jurassic basin. Zato et al. (2011) have postulated that the Bathonian concretions were formed by early diagenetic processes just below the sediment-water interface during low sedimentation rate episodes. They were repeatedly exhumed, overturned and moved on the sea floor probably due to episodic storm-related bottom cur-

rents in shallow sub-tidal environments. The carbonate concretions in the Wolica section were probably formed in similar conditions. The algal coatings, fragments of bryozoans, bivalve shells and single borings on their surfaces record episodes of high-energy conditions in marine environments with a generally low energy and low sedimentation rate.

CONCLUSIONS

The topmost part of the Upper Triassic succession in the Wolica section differs from the underlying rocks in the presence of a considerable proportion of fluvial deposits. The fluvial system was linked with the infilling of channels with an almost latitudinal strike. The dip of the cross-bedding indicates the dominance of northwestern transport directions in the Late Triassic. This sedimentary pattern change suggests the decrease of accommodation space continuing into the uppermost part of the Triassic succession, which contains numerous weathering surfaces and probably significant depositional breaks. In the context of the history of the local basin, the observed evolution, from an active depocentre towards an area with active erosion, may be interpreted as caused by tectonic uplift of the Wolica area in relation to the basin axis located to the north. Rising palaeorelief across the Triassic–Jurassic transition and tectonic activation is documented by the presence of the Snochowice Beds and their thickness/facies pattern of alluvial fan origin. Their accumulation was associated directly with the tectonic activity of the basement during Late Triassic–Early Jurassic times (Pie kowski, 2004; Bra ski, 2004; Kozłowska, 2012). Tectonic movements were also reported by other authors (e.g., Jurkiewiczowa, 1967; Deczkowski and Franczyk, 1988) based on the variable depth of Late Triassic–Early Jurassic erosion in different parts of the western MHCM.

Waning deposition documented by numerous weathering surfaces in the top of the Upper Triassic strata in the section studied indicates the lack of continuity of deposition in the Late Norian and Rhaetian. Based on the observed succession of facies, the Late Norian–Rhaetian sedimentation in the southern MHCM was limited only to low ground (as documented by Pawłowska, 1979), especially in palaeovalleys.

The red Upper Triassic deposits in the succession studied are overlain by a yellowish-green mudstone succession of unknown age (Unit 2a). The occurrence of this unit above the Upper Triassic mudstone succession with numerous weathered surfaces suggests that the rocks may represent a relic of an independent, transgressive sedimentary event, which must have occurred after the Late Triassic sedimentation cycle. They can represent any of the transgressive events between the late Norian and Late Bajocian. One of the possible events may have been the late Early Jurassic marine incursion (Early Pliensbachian or Early Toarcian) described by Pie kowski (2004), or an Early Bajocian transgression pulse, widely recorded in the Cz stochowa region as the Ko cieliskie Beds (Kopik, 1998); however, future biostratigraphical studies of this rock interval are required to resolve this issue.

The main Middle Jurassic transgressive event above the stratigraphic gap is dated at the Bajocian–Bathonian transition (Unit 2b). A delayed marine incursion in relation to adjacent areas, where the transgression took place in the Early Bajocian or even Aalenian (Kraków–Wielu region, Nida Trough and north

of the MHCM), suggest that the study area represents an intrabasinal elevation, which may have had an island character during the beginning of marine flooding. The transport directions recorded in the fluvial-marginal marine sandy unit at Wolica indicate that the elevation was located to the north of the present lateral extent of Jurassic rocks – at present the area of the HCM Fold Belt.

The upper part of sandy Unit 2b contains fresh-water algal fossils, which indicate the evolution of the sedimentary environment towards a marginal marine environment. The Middle Jurassic sea transgressed on to a relatively flat land locally from the south, however, probably cut by minor fluvial valleys, possibly with a local NNW–SSE strike. The oldest transgressive deposits are associated with the rise of the erosive base that resulted in sedimentary fills of the palaeovalleys, evolving from riverine to marginal marine, probably estuarine sedimentary environments, formed in the mouths of the palaeovalleys.

Further progress of transgression on a flat/low-relief land caused its overall flooding, which may have caused significant starvation of the local basin, recorded as a distinct gap represented by the hiatus bed with carbonate concretions. In the case of synchronous flooding of the local hinterland, this hiatus horizon may have a potential for local correlation.

The sandstone lithosomes in the basal part of the succession that were recently exposed in Wolica are similar to the Ko cieliskie Beds, known from another part of the Polish Basin, the Cz stochowa region (Kopik, 1998). Siliciclastic deposits of Lower Bajocian age underlie the Ore-Bearing Cz stochowa Clay Formation and document the beginning of the Middle Jurassic transgression in the southernmost part of the Polish Basin.

The diachronous Middle Jurassic transgression is also discernible by means of dinoflagellate cysts. More diverse and prolific assemblages are observed as the section is ascended, with increasing dominance of *Ctenidodinium* spp. especially *C. combazii*. High abundances of this genus and species, according to Fenton and Fisher (1978), characterize Tethyan realm assemblages. They noted northward migration of this species during the Bathonian transgressive phase in NW Europe. High frequencies of *Ctenidodinium combazii* in the uppermost samples may also reflect marine connections between the study area and the Tethyan Ocean at this time.

Acknowledgements. We would like to thank the reviewers of this paper: Prof. P. Tucholka, Dr. hab. G. Pie kowski and one anonymous reviewer for their constructive comments. We would like to express warmest acknowledgements to Prof. B.A. Matyja for his many and very helpful discussions during the research. Special thanks go to Dr. W. Kozłowski for reporting the newly exposed Wolica section and later for many perceptive discussions during the preparation of the manuscript. This work was supported by the internal grants system of the Institute of Geology, Faculty of Geology, University of Warsaw.

REFERENCES

- Baines, D., Smith, D.G., Froese, D.G., Bauman, P., Nimeck, G., 2002. Electrical resistivity ground imaging (ERGI): a new tool for mapping the lithology and geometry of channel-belts and valley-fills. *Sedimentology*, **49**: 441–449.
- Barski, M., 1999. Dinocyst stratigraphy of the Jurassic black clays from Holy Cross Mts area (Central Poland) (in Polish with English summary). *Przeł d Geologiczny*, **47**: 718–722.

- Bra ski, P., 2004.** Formacja zagajska w regionie wi tokrzyskim – zapis zdarzenia tektonicznego na przełomie triasu i jury (in Polish). *Tomy Jurajskie*, **2**: 161–162.
- Cie li ski, S., Po aryski, W., 1970.** Cretaceous (in Polish with English summary). *Prace Instytutu Geologicznego*, **56**: 185–231.
- Czarnocki, J., 1927.** Compte-rendu des recherches exécutées en 1926 et la structure de Mésozoïque de la région de Chęciny (in Polish with French summary). *Posiedzenia Naukowe Pa stwowe Instytutu Geologicznego*, **17**: 4–14.
- Czarnocki, J., 1938.** Mapa geologiczna Polski 1:100 000, arkusz 4, Kielce (in Polish). Pa stwowy Instytut Geologiczny, Warszawa.
- Dadlez, R., 1962.** Equivalents of the Polomia Beds of the Cz stochowa Lias in the wesern margin area of the wi ty Krzy Mountains (in Polish with English summary). *Kwartalnik Geologiczny*, **6** (3): 447–458.
- Dalrymple, R.W., Choi, K., 2007.** Morphologic and facies trends through the fluvial-marine transition in tide-dominated depositional systems: a schematic framework for environmental and sequence-stratigraphic interpretation. *Earth-Science Reviews*, **81**: 135–174.
- Daniec, J., 1970.** Middle Jurassic (in Polish with English summary). *Prace Instytutu Geologicznego*, **56**: 99–133.
- Dayczak-Calikowska, K., Moryc, W., 1988.** Evolution of sedimentary basin and paleotectonics of the Middle Jurassic in Poland (in Polish with English summary). *Kwartalnik Geologiczny*, **32** (1): 117–136.
- Deczkowski, Z., Franczyk, M., 1988.** Paleothickness, lithofacies and paleotectonics of the Norian and Rhaetian in Polish Lowland (in Polish with English summary). *Kwartalnik Geologiczny*, **32** (1): 93–104.
- Deczkowski, Z., 1997.** Norian–Rhaetian (in Polish with English summary). *Prace Pa stwowe Instytutu Geologicznego*, **153**: 174–184.
- Feist-Burkhardt, S., 1994.** Stratigraphic compilation of Below's data (1987a, 1987b and 1990) on Early and Middle Jurassic dinoflagellate cysts. *Revue de Paléobiologie*, **13**: 313–318.
- Feldman-Olszewska, A., 1997.** Depositional architecture of the Polish epicontinental Middle Jurassic basin. *Geological Quarterly*, **41** (4): 491–508.
- Fenton, J.P.G., Fisher, M.J., 1978.** Regional distribution of marine microplankton in the Bajocian and Bathonian of north-west Europe. *Palínologia, número extraordinario*, **1**: 233–243.
- Fijałkowska, A., 1992.** Palynostratigraphy of the Keuper and Rhaetic in north-western margin of the Holy Cross Mts. *Geological Quarterly*, **36** (2): 199–220.
- Fijałkowska-Mader, A., 2013.** Palynostratigraphy, palaeoecology and palaeoclimate of the Late Permian and Triassic Nida Basin (in Polish with English summary). *Biuletyn Pa stwowe Instytutu Geologicznego*, **454**: 15–70.
- Fijałkowska-Mader, A., 2015.** Record of climatic changes in the Triassic palynological spectra from Poland. *Geological Quarterly*, **59** (4): 615–653.
- Filonowicz, P., 1965.** Baton w okolicy Woli Morawickiej (in Polish). *Kwartalnik Geologiczny*, **9** (4): 946–947.
- Filonowicz, P., 1966.** Szczegółowa mapa geologiczna Polski 1:50 000, arkusz Nowa Słupia (in Polish). *Wyd. Geol., Warszawa*.
- Filonowicz, P., 1967.** Szczegółowa mapa geologiczna Polski 1:50 000, arkusz Morawica (in Polish). *Wyd. Geol., Warszawa*.
- Filonowicz, P., 1973.** Szczegółowa mapa geologiczna Polski 1:50 000, arkusz Kielce wraz z obja nieniami (in Polish). *Wyd. Geol., Warszawa*.
- Filonowicz, P., 1976.** Szczegółowa mapa geologiczna Polski 1:50 000, arkusz Daleszyce wraz z obja nieniami (in Polish). *Wyd. Geol., Warszawa*.
- Gajewska, I., Deczkowski, Z., Maliszewska, A., Marcinkiewicz, T., 1997.** Upper Triassic (in Polish with English summary). *Prace Pa stwowe Instytutu Geologicznego*, **153**: 151–194.
- Giocoli, A., Magri, C., Vannoli, P., Piscitelli, S., Rizzo, E., Siniscalchi, A., Burrato, P., Basso, C., Di Nocera, S., 2008.** Electrical Resistivity Tomography investigations in the Ufita Valley (Southern Italy). *Annals of Geophysics*, **51**: 213–223.
- Guy-Ohlson, D., 1992.** Botryococcus as an aid in the interpretation of palaeoenvironment and depositional processes. *Review of Palaeobotany and Palynology*, **71**: 1–15.
- Hakenberg, M., 1973.** Szczegółowa mapa geologiczna Polski 1:50 000, arkusz Ch ciny (in Polish). *Wyd. Geol., Warszawa*.
- Hakenberg, M., 1974.** Obją nienia do Szczegółowej mapy geologicznej Polski 1:50 000, arkusz Ch ciny (in Polish). *Wyd. Geol., Warszawa*: 1–84.
- Hornung, J., Aigner, T., 1999.** Reservoir and aquifer characterization of fluvial architectural elements: Stubensandstein, Upper Triassic, southwest Germany. *Sedimentary Geology*, **129**: 215–280.
- Jurkiewicz, H., 1974.** Development of the Triassic in the central area of the Nida Trough (in Polish with English summary). *Kwartalnik Geologiczny*, **18** (1): 90–108.
- Jurkiewiczowa, I., 1967.** The Lias of the western part of the Mesozoic zone surrounding the wietokrzyskie (Holy Cross) Mountains and its correlation with the Lias of the Cracow-Wielu Range (in Polish with English summary). *Biuletyn Instytutu Geologicznego*, **200**: 5–132.
- Karaszewski, W., 1962.** The stratigraphy of the Lias in the northern Mesozoic Zone surrounding the wi ty Krzy Mountains (Central Poland) (in Polish with English summary). *Prace Instytutu Geologicznego*, **30**: 333–416.
- Karaszewski, W., Kopik, J., 1970.** Lower Jurassic (in Polish with English summary). *Prace Instytutu Geologicznego*, **56**: 65–98.
- Kasprzak, M., Traczyk, A., 2014.** LiDAR and 2D electrical resistivity tomography as a supplement of geomorphological investigations in urban areas: a case study from the city of Wrocław (SW Poland). *Pure and Applied Geophysics*, **171**: 835–855.
- Kirsch, R., 2009.** Groundwater Geophysics, a Tool for Hydrogeology. Springer, Berlin.
- Konon, A., 2007.** Strike-slip faulting in the Kielce Unit, Holy Cross Mountains, central Poland. *Acta Geologica Polonica*, **57**: 415–441.
- Kopik, J., 1970.** Rhaetian (in Polish with English summary). *Prace Instytutu Geologicznego*, **56**: 49–63.
- Kopik, J., 1998.** Lower and Middle Jurassic of the north-eastern margin of the Upper Silesian Coal Basin (in Polish with English summary). *Biuletyn Pa stwowe Instytutu Geologicznego*, **378**: 67–116.
- Kozłowska, M., 2012.** Sedimentary environment and tectonic controls of the Snochowice Beds (Lower Jurassic, western margin of the Holy Cross Mountains, Poland). *Geological Quarterly*, **56** (2): 299–314.
- Krupnik, J., Ziaja, J., Barbacka, M., Feldman-Olszewska, A., Jarzynka, A., 2014.** A palaeoenvironmental reconstruction based on palynological analyses of Upper Triassic and Lower Jurassic sediments from the Holy Cross Mountains region. *Acta Palaeobotanica*, **54**: 35–65.
- Kutek, J., Głazek, J., 1972.** The Holy Cross area, central Poland in the Alpine cycle. *Acta Geologica Polonica*, **22**: 603–653.
- Leckie, D.A., Singh, C., 1991.** Estuarine deposits of the Albian Paddy Member (Peace River Formation) and lowermost Shaftesbury Formation, Alberta, Canada. *Journal of Sedimentary Petrology*, **61**: 825–849.
- Leonowicz, P., 2013.** The significance of mudstone fabric combined with palaeoecological evidence in determining sedimentary processes – an example from the Middle Jurassic of southern Poland. *Geological Quarterly*, **57** (2): 243–260.
- Lewi ski, J., 1912.** Les dépôts jurassiques du versant occidental des montagnes de wi ty Krzy (in Polish with French summary). *Sprawozdanie Towarzystwa Naukowego Warszawskiego*, **5**: 501–599.
- Loke, M.H., 2012.** Tutorial: 2-D and 3-D Electrical Imaging Surveys. Geotomo Software, Malaysia.
- Loke, M.H., Chambers, J.E., Rucker, D.F., Kuras, O., Wilkinson, P.B., 2013.** Recent developments in the direct-current geoelectrical imaging method. *Journal of Applied Geophysics*, **95**: 135–156.
- Love, S., Williams, B.P.J., 2000.** Sedimentology, cyclicity and floodplain architecture in the Lower Old Red Sandstone of SW Wales. *Geological Society Special Publications*, **180**: 371–388.

- Marcinkiewicz, T., Orłowska-Zwolińska, T., 1985.** Co-occurrence of the *Corollina meyeriana* miospore assemblage and megaspore *Striatriletes ramosus* sp. in the uppermost Triassic of Poland (in Polish with English summary). *Kwartalnik Geologiczny*, **29** (3–4): 691–712.
- Marcinkiewicz, T., Orłowska-Zwolińska, T., 1994.** Miospores, megaspores and *Lepidopteris ottonis* (Goeppert) Schimper in the uppermost Triassic deposits from Poland. *Geological Quarterly*, **38** (1): 97–116.
- Marcinkiewicz, T., Fijałkowska-Mader, A., Piekosiński, G., 2014.** Megaspore zones of the epicontinental Triassic and Jurassic deposits in Poland – overview (in Polish with English summary). *Biuletyn Państwowego Instytutu Geologicznego*, **457**: 15–42.
- Matyja, A., 1977.** The Oxfordian in the south-western margin of the Holy Cross Mts. *Acta Geologica Polonica*, **27**: 41–64.
- Matyja, A., 2015.** Jurassic evolution of the northern margin of the Tethys Ocean (in Polish). In: *Przewodnik LXXXIV Zjazdu Naukowego PTG*, 9–11.09.2015: 28–40.
- Miall, A.D., 1996.** The Geology of Fluvial Deposits. Sedimentary Facies, Basin Analysis, and Petroleum Geology. Springer-Verlag.
- Newell, A.J., Tverdokhlebov, V.P., Benton, M.J., 1999.** Interplay of tectonics and climate on a transverse fluvial system, Upper Permian, Southern Uralian Foreland Basin, Russia. *Sedimentary Geology*, **127**: 11–29.
- Orłowska-Zwolińska, T., 1983.** Palynostratigraphy of the upper part of Triassic epicontinental sediments in Poland (in Polish with English summary). *Prace Instytutu Geologicznego*, **104**: 1–89.
- Pawłowska, K., 1979.** Triassic rocks of south-eastern Góry Wierzbne Mts (in Polish with English summary). *Kwartalnik Geologiczny*, **23** (2): 337–361.
- Penland, S., Boyd, R., Suter, J.R., 1988.** Transgressive depositional systems of the Mississippi Delta plain; a model for barrier shoreline and shelf sand development. *Journal of Sedimentary Research*, **58**: 932–949.
- Piekosiński, G., 1983.** Early Lias sedimentary environments at northern margin of the Holy Cross Mts (in Polish with English summary). *Przebieg Geologiczny*, **31**: 223–230.
- Piekosiński, G., 2004.** The epicontinental Lower Jurassic of Poland. *Polish Geological Institute Special Papers*, **12**: 1–154.
- Piekosiński, G., 2009.** Triassic. In: *Supplement to Stratigraphy Table of Poland* (ed. R. Wagner): 50–51. Państwowy Instytut Geologiczny.
- Piekosiński, G., Schudack, M.E., Bosák, P., Enay, R., Feldman-Olszewska, A., Golonka, J., Gutowski, J., Henggreen, G.F.W., Jordan, P., Krobicki, M., Lathuiliere, B., Leinfelder, R.R., Michalik, J., Mönnig, E., Noe-Nygaard, N., Pálffy, J., Pint, A., Rasser, M.W., Reisdorf, A.G., Schmid, D.U., Schweigert, G., Surdyk, F., Wetzel, A., Wong, T.E., 2008.** Jurassic. In: *The Geology in Central Europe, Volume 2 – Mesozoic and Cenozoic* (ed. T. McCann): 823–922. The Geological Society of London.
- Piekosiński, G., Niedźwiedzki, G., Barski, P., 2014.** CAMP-related rapid climatic reversals caused the end-Triassic biota crisis – evidence from continental strata in Poland. *GSA Special Papers*, **505**: 263–286.
- Poulsen, N.E., 1998.** Bajocian to Callovian (Jurassic) dinoflagellate cysts from central Poland. *Acta Geologica Polonica*, **48**: 237–245.
- Poulsen, N.E., Riding, J.B., 2003.** The Jurassic cyst zonation of Subboreal Northwest Europe. *Geological Survey of Denmark and Greenland Bulletin*, **1**: 115–144.
- Prauss, M., 1989.** Dinozysten-stratigraphie und Palynofazies imoberen Lias und Dogger von NW-Deutschland. *Palaeontographica*, Abt. B, **214**: 1–124.
- Radwanski, A., 1969.** Lower Tortonian transgression onto the southern slopes of the Holy Cross Mts. (in Polish with English summary). *Acta Geologica Polonica*, **19**: 1–164.
- Radwanski, A., 1973.** Lower Tortonian transgression onto the south-eastern and eastern slopes of the Holy Cross Mts. (in Polish with English summary). *Acta Geologica Polonica*, **23**: 375–434.
- Riding, J.B., Thomas, J.E., 1992.** Dinoflagellate cysts of the Jurassic system. In: *A Stratigraphic Index of Dinoflagellate Cysts* (ed. A.J. Powell): 7–57. Chapman and Hall, London.
- Rossetti, D.F., Netto, R.G., 2006.** First evidence of marine influence in the Cretaceous of the Amazonas Basin, Brazil. *Cretaceous Research*, **27**: 513–528.
- Senkowińska, H., 1970.** Triassic (without Rhaetian deposits) (in Polish with English summary). *Prace Instytutu Geologicznego*, **56**: 7–48.
- Siemińska, M., 1967.** Nowe odsłonięcia kontaktu kajpru i doggeru w Woli Morawickiej (in Polish). *Przebieg Geologiczny*, **15**: 82–83.
- Siemińska, M., 1969.** The transgressive Callovian deposits at Gumienice, southern Mesozoic margin of the Holy Cross Mts. (in Polish with English summary). *Acta Geologica Polonica*, **19**: 165–174.
- Siemińska-Giejewska, M., 1970.** Stratigraphy and sedimentation of the Middle Jurassic in the south-western margin of the Holy Cross Mountains (in Polish). Unpublished Ph.D thesis, Faculty of Geology, University of Warsaw.
- Siemińska-Giejewska, M., 1974.** Stratigraphy and paleontology of the Callovian in the southern and western margins of the Holy Cross Mountains. *Acta Geologica Polonica*, **24**: 365–406.
- Stover, L.E., Brinkhuis, H., Damassa, S.P., de Verteuil, L., Helby, R.J., Monteil, E., Partridge, A.D., Powell, A.J., Riding, J.B., Smelror, M., Williams, G.L., 1996.** Mesozoic-Tertiary dinoflagellates, acritarchs and prasinophytes. *American Association of Stratigraphic Palynologists Foundation*, **2**: 641–750.
- Szulc, J., 2000.** Middle Triassic evolution of the northern Peritethys area as influenced by early opening of the Tethys Ocean. *Annales Societatis Geologorum Poloniae*, **70**: 1–48.
- Szulczewski, M., 1967.** Stromatolitic structures within Middle Jurassic transgressive deposits at Wola Morawicka (southern margins of the Holy Cross Mountains, Central Poland) (in Polish with English summary). *Rocznik Polskiego Towarzystwa Geologicznego*, **37**: 515–528.
- Trammer, J., 1975.** Stratigraphy and facies development of the Muschelkalk in the south-western Holy Cross Mts. *Acta Geologica Polonica*, **25**: 179–216.
- Woollam, R., Riding, J.B., 1983.** Dinoflagellate cyst zonation of the English Jurassic. *Institute of Geological Sciences Report*, **83**: 1–41.
- Zatoń, M., Machocka, S., Wilson, M.A., Marynowski, L., Taylor, P.D., 2011.** Origin and paleoecology of Middle Jurassic hiatus concretions from Poland. *Facies*, **57**: 275–300.
- Żelaźnicki, A., Aleksandrowski, P., Buła, Z., Karnkowski, P.H., Konon, A., Oszczytko, N., Iliczka, A., Jaba, J., Ytko, K., 2011.** Regionalizacja tektoniczna Polski (in Polish). *Komitet Nauk Geologicznych PAN, Wrocław*.
- Zieliński, T., 1998.** Litofacyjna identyfikacja osadów rzecznych (in Polish). In: *Sedymentacyjne i postsedymentacyjne struktury osadów czwartorzędowych i ich wartość interpretacyjna* (ed. E. Mycielska-Dowgiałło): 195–251. Uniwersytet Warszawski.